Asia Pacific Research Initiative for Sustainable Energy Systems 2011 (APRISES11)

Office of Naval Research
Grant Award Number N0014-12-1-0496

OTEC Heat Exchanger Development and Testing

Task 4.1

Prepared For

Hawaii Natural Energy Institute

1680 East West Road, POST 109

Honolulu, HI, 96822

Prepared By

MAKAI OCEAN ENGINEERING

PO Box 1206, Kailua, Hawaii 96734

December 2014

HNEI
Hawai‘i Natural Energy Institute
University of Hawai‘i at Mānoa

OTEC HX TESTING PROGRAM
2014 ANNUAL REPORT

Prepared For

HAWAII NATURAL ENERGY INSTITUTE

RICK ROCHELEAU

1680 East West Road, POST 109

Honolulu, HI, 96822

USA

Prepared By

MAKAI OCEAN ENGINEERING

PO Box 1206, Kailua, Hawaii 96734

December 2014

1. EXECUTIVE SUMMARY

Makai Ocean Engineering, Inc.'s Ocean Thermal Energy Conversion (OTEC) Heat Exchanger (HX) Testing program at the Ocean Energy Research Center (OERC) is focused on developing an economically viable OTEC power plant. Heat exchangers are one of the most expensive components in an OTEC power plant; proper heat exchanger selection is crucial to the economic viability of OTEC. Heat exchanger development must balance size, cost, and performance. To meet this goal, the OTEC HX Testing Program is divided into three areas: HX Performance Testing, HX Design Development, and Corrosion Testing. This report reviews Makai's activities and summarizes the completion of the Milestones under APRISES11, conducted from **March 2013 to December 2014**.

Major accomplishments in this period include:

HX Performance Testing Facility

- Facility used to complete performance testing of APV Titanium Plate-Frame Heat Exchanger, APV Cross Flow Heat Exchanger, and Lockheed Horizontal Heat Exchanger.
- Modifications completed in preparation for turbine installation and testing.
- Upgraded instrumentation and instrument wiring on the facility.
- New revision to the control software.
- Completion of 100-kW Testing Station.

HX Design Development

- APV Titanium Plate-Frame Heat Exchanger was designed, fabricated, installed, and performance tested.
- APV Cross-Flow Heat Exchanger was designed, fabricated, installed, and performance tested.
- Lockheed Martin Horizontal Evaporator was designed, fabricated, installed, and performance tested.

Corrosion Testing

- Removal and analysis of 4-year hollow extrusion corrosion samples.
- Ongoing testing of pit mitigation treatments.
- Completed testing of alternative treatments to prevent biofouling.
- Completed coatings testing.
- Installed Lockheed Martin representative heat exchanger samples and plate samples for the multi-column imaging rack (MCIR) – included warm seawater pre-treatment for several samples.

Major findings in this period include:

HX Testing Facility

- No major findings.

HX Design

- APV Titanium Plate-Frame Heat Exchanger had high overall heat transfer coefficient and very high seawater side pressure drop.
- APV Cross Flow Evaporator had average overall heat transfer coefficient and very low seawater side pressure drop.

Corrosion Testing

- Hypochlorination is the most effective biofoulant control.
- Siloxel and Alodine coatings provide protection but coating uniformity was unreliable and therefore, corrosion protection was limited.
- Steel is no longer being pursued as a potential material for a condenser.
- Pit mitigation treatments should be performed based on the sample's open circuit potential (OCP), not set intervals.

2. HX PERFORMANCE TESTING FACILITY

As of October 2014, the HX Performance Testing Facility is at capacity with six heat exchangers installed. On the condenser side, the Lockheed Martin Shell and Tube Heat Exchanger, Lockheed Martin Enhanced Tube Heat Exchanger, and the APV Titanium Plate-Frame Heat Exchanger are installed. On the evaporator side, CHART's Brazed Aluminum Heat Exchanger, Lockheed Martin's Horizontal Shell and Tube Heat Exchanger, and APV's Cross-Flow Heat Exchanger are installed.

Facility instrumentation was upgraded to include new ultra-sonic seawater flow sensors, an additional liquid ammonia Coriolis flow meter in the separator-receiver line, a level sensor in the separator-receiver line, and a pair of precise temperature probes for during heat exchanger testing. Instrument wiring was overhauled in June 2014 with new conduit, junction boxes, multi-conductor cabling, and standardized terminal blocks. A positive pressure system was also installed to supply dry compressed air to aid in keeping instrumentation dry. Instrument calibration was performed in August and September 2014. Pressure, temperature, and flow sensors were calibrated in preparation for upcoming HX performance testing.

3. HX DESIGN AND DEVELOPMENT

Makai completed designs for two APV titanium plate-frame style heat exchangers. Both have been tested at the HX Performance Testing Facility. A Lockheed Martin Horizontal Shell and Tube Heat Exchanger was also tested at the HX Performance Testing Facility during this period.

The key parameters of heat exchanger performance that directly affect OTEC plant design are overall heat transfer coefficient, seawater-side pressure drop, and ammonia-side pressure drop. The overall heat transfer coefficient (U) is a measure of the heat exchanger's efficiency. Heat exchangers with higher U values require less surface area to transfer a given duty. This is important for OTEC because more efficient heat exchangers require less space which equates to big savings on the cost of the remoras. The ammonia-side and seawater-side convective heat transfer coefficients were also calculated using the definition of the overall heat transfer coefficient as a function of the convective and conductive heat transfer coefficients. h_1 and h_2 are the ammonia-side and water-side convective heat transfer coefficients, k is the conductivity of aluminum and dx is the wall thickness of the titanium plate extrusion.

$$U = 1/(1/h_1 + dx_w/k + 1/h_2)$$

In order to determine h_1 and h_2, the water-side heat transfer coefficient was assumed to be constant for each water flow rate set point and the ammonia-side heat transfer coefficient was assumed to be constant for each duty set point. The method of least squares was then used to determine a single heat transfer coefficient for each set point.

Seawater-side pressure drop affects the amount of OTEC-generated power that must be used to supply seawater pumps on an OTEC plant. High pressure drops require large amounts of pumping power, which reduces the net-power output from the OTEC plant. Ammonia-side pressure drop is not expected to be a significant factor.

Ammonia-side operating pressure and approach temperature also provide valuable insight to heat exchanger performance and further our understanding of design decisions. Ammonia-side operating pressure is related to power production because the power generated in an OTEC plant is a function of the pressure drop across the turbine and the ammonia flow rate. A lower pressure on the condenser side and higher pressure on the evaporator side is generally better for OTEC as this increases the pressure drop across the turbine and creates higher power output. Approach temperature is the difference in temperature of the two fluids at the heat exchanger outlet. Small approach temperatures indicate the amount of heat transferred toward the end of the heat exchanger is greatly diminished due to small temperature differences between the two fluids.

3.1. APV TITANIUM PLATE-FRAME HEAT EXCHANGER

The APV titanium plate-frame heat exchanger was designed and tested as a condenser. APV and Makai worked together to customize the design for OTEC conditions. In a plate-frame heat exchanger, fluid flows in channels between a series of stacked plates. Gaskets are used to seal the plates. A rigid steel frame is used to hold the plates together and maintain gasket compression. Each plate has a port in two opposing corners to allow either hot or cold fluid to enter. The use of larger plates in the APV condenser (plates are larger than plates in existing plate-frame heat exchangers that Makai has researched) allows for fewer manifold pipes in a full-scale OTEC power plant. Titanium was selected as a low-risk solution for a condenser. Pitting, which has been observed in corrosion testing of aluminum alloys, remains a concern regarding the longevity of aluminum condensers, especially in cold seawater. Although the initial cost of a titanium heat exchanger is more than a comparable aluminum heat exchanger, the aluminum heat exchanger may not last the life of an OTEC plant and required additional maintenance and replacement costs.

Table 3-1. APV Titanium Plate-Frame Heat Exchanger Specifications

Plate Properties	
Material	Titanium ASTM B265 Grade1
Number of Plates	97 total
Plate Thickness	0.5 mm
Total heat transfer area	214.89 m^2 total

Frame Properties	
Material	Carbon Steel
Frame Height	3.74 m
Frame Width	1.28 m
Frame Length	3.30 m
Max Number of Plates Pairs	48 + 1 single

The APV condenser arrived in the OERC on October 14, 2013 and was installed over a ten-day span. Performance testing was conducted on October 28, 2013. A total of 19 operating points were tested (Table 3-2). Each operating point was held at steady state for at least ten minutes. Steady state was defined as being within +/- 3% for duty, +/- 2% for seawater flow rate, +/- 0.1°C for seawater inlet temperature, +/-0.2°C for seawater temperature difference, +/- 2% for LMTD, +/- 2% for ammonia flow rate, +/- 2% for quality, and +/- 1 kPa for condenser pressure.

Figure 3-1. APV Titanium plate-frame heat exchanger installed on the OERC HX Performance Testing Facility.

Table 3-2. APV Condenser Performance Testing Points

Cold Water Flow [gpm]		Duty [kW] 1000	1500	2000	2500	3000
	1000	X	X	X		
	1500	X	X	X	X	
	2000	X	X	X	X	
	2500		X	X	X	X
	2900		X	X	X	X

3.1.1. Overall heat transfer coefficient

U is plotted below in two ways – with lines of constant seawater flow and with lines of constant duty. U is mostly dependent on water velocity and less dependent on duty, indicating the heat exchanger is limited by the water-side heat transfer rate.

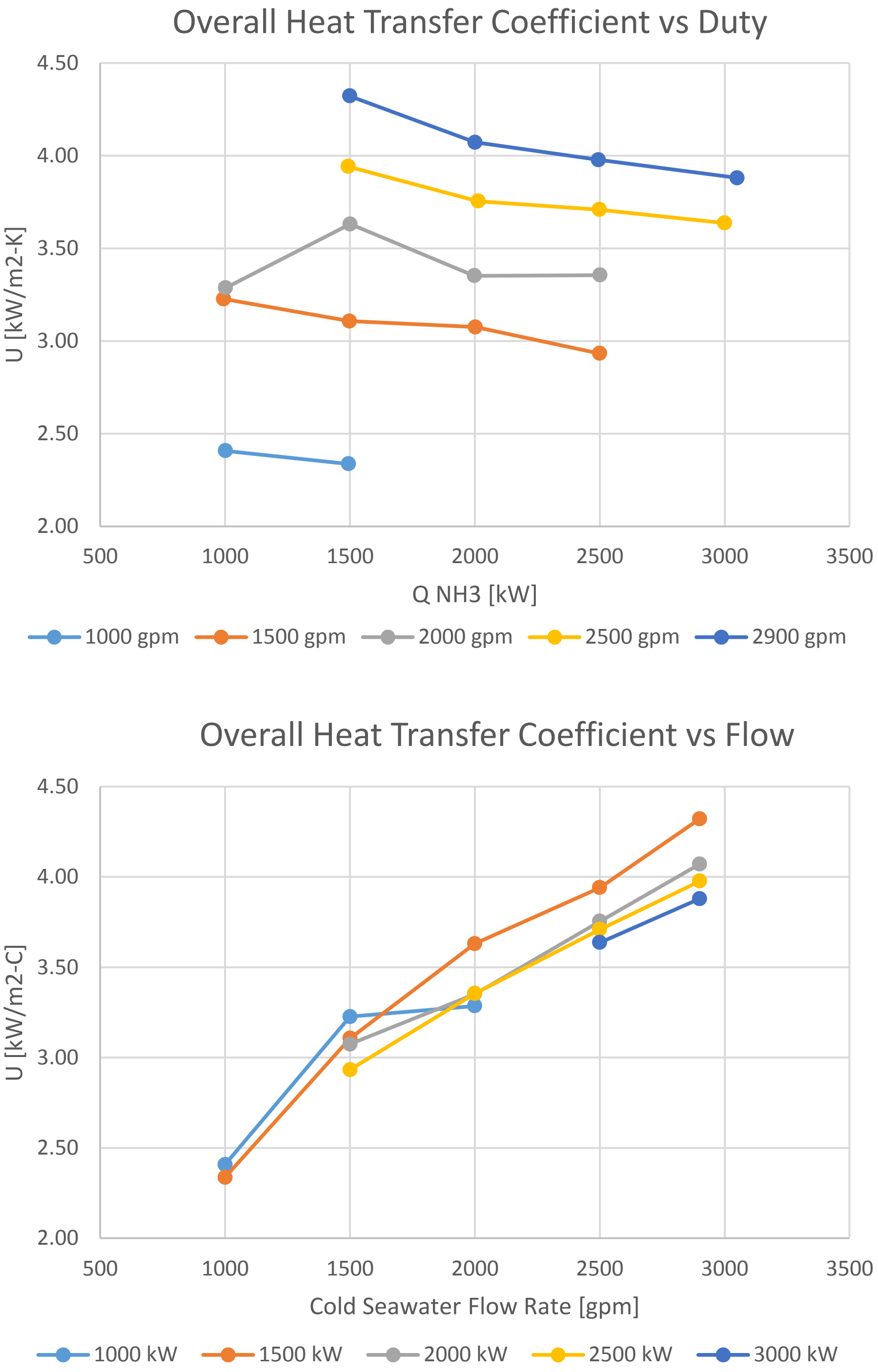

Figure 3-2. Condenser overall heat transfer coefficient

3.1.2. Convective heat transfer coefficient

In the tested range, the overall heat transfer coefficient was mainly influenced by the seawater convective heat transfer coefficient which varied from 4 to 14 kW/m^2-C whereas the ammonia convective heat transfer coefficient showed little change (6.5 to 7.5 kW/m^2-C).

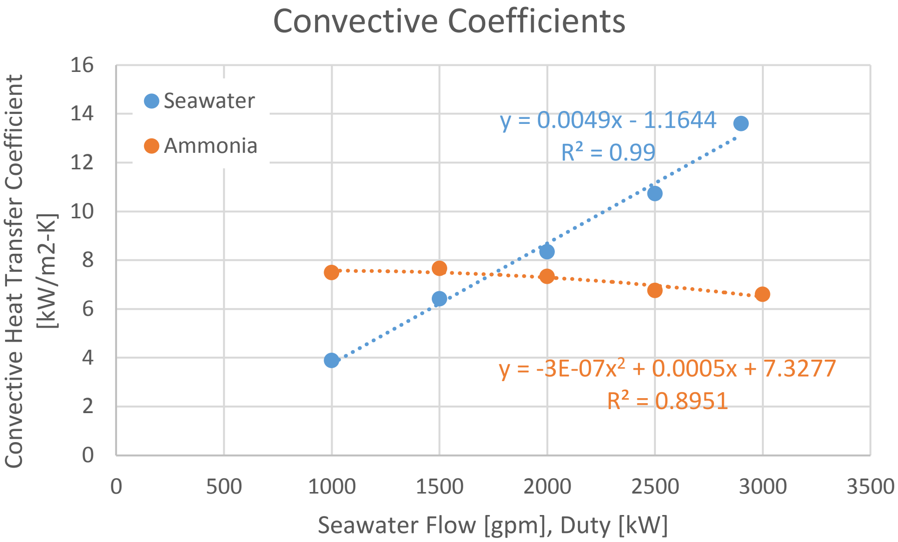

Figure 3-3. Ammonia and seawater convective heat transfer coefficients fitting the equation $1/U = 1/h_{sw} + dx_w/k + 1/h_{NH3}$ solved for using the least–squares method.

3.1.3. Seawater-side pressure drop

The seawater-side pressure drop is independent of duty and has a power-law relationship to water velocity. The power-law relationship has an exponent of ~2.7. Pressure drop increases exponentially with increased water flow, opposite to the trend of U value, which shows diminishing increases with increased flow. These opposing trends imply there is an optimum water velocity that balances increased U value with increased pressure drop across the condenser.

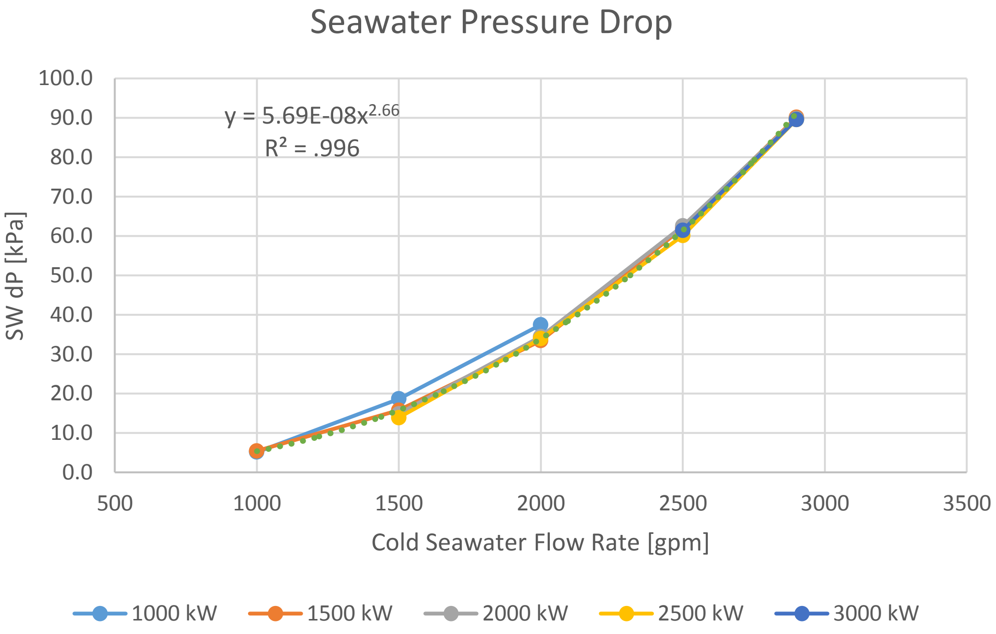

Figure 3-4. Seawater-side pressure drop

3.1.4. Ammonia-side pressure drop

The magnitude of the pressure drop on the ammonia side is much smaller than the pressure drop on the seawater side. Also, one of the ammonia pressure sensors may be faulty – the dP across the condenser should never be negative.

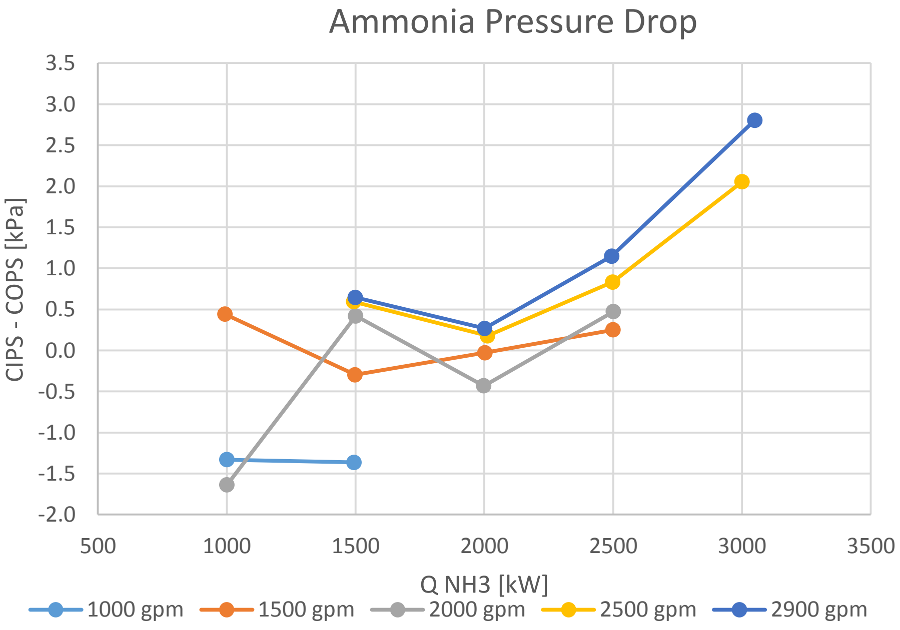

Figure 3-5. Ammonia-side pressure drop

3.1.5. Ammonia-side operating pressure

For a given duty, the condenser pressure decreases with increased seawater flow rate. This means that the power output should be greater for higher water flow rates. However, the increased power with increasing seawater flow will eventually be offset by the increased pumping power at higher flows (due to the increase in seawater-side pressure drop).

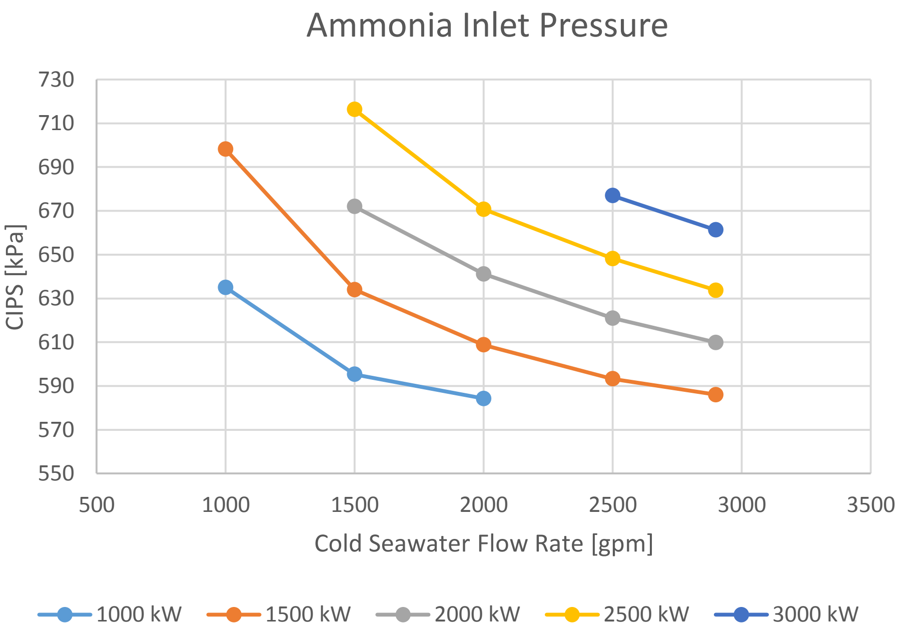

Figure 3-6. Ammonia absolute pressure at condenser inlet

3.1.6. Approach Temperature

Ammonia duty is used in this calculation because the ammonia pressure sensors are used to calculate the ammonia temperature at saturation and provide a more accurate temperature measurement than the temperature sensors on the seawater side.

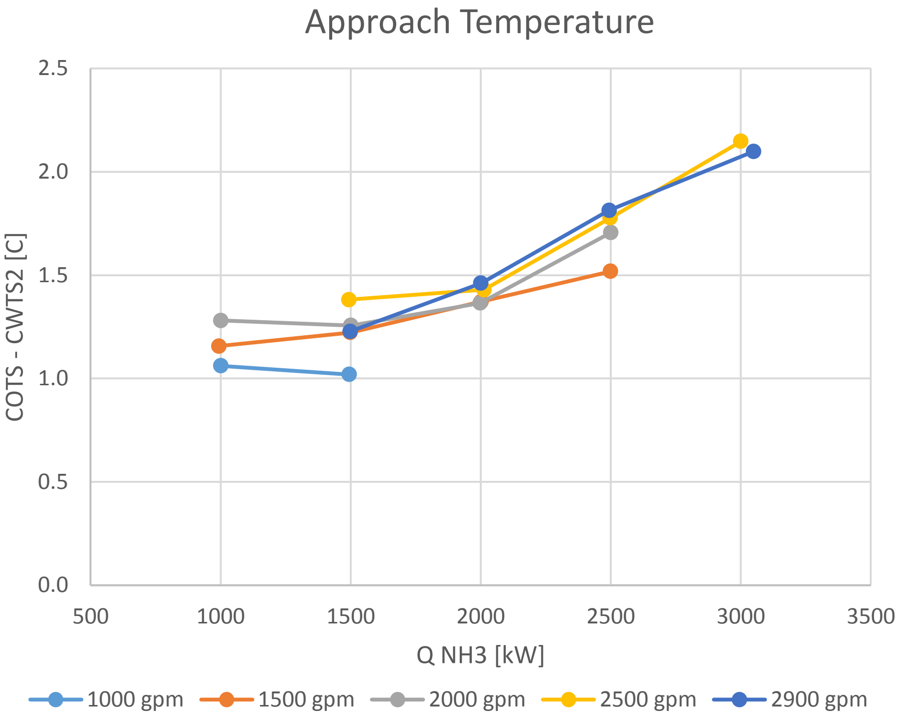

Figure 3-7. Approach temperature

The data shows a linear relationship between duty and approach temperature, with the slope of the line dependent on the water velocity. The approach temperature increases with duty because higher duty corresponds to higher ammonia operating pressure, and thus a higher saturation temperature.

3.1.7. Difference between ammonia and seawater duty

Theoretically, if the condenser was perfectly insulated, the ammonia duty should be identical to the seawater duty. However, during testing heat from the outside environment and sensor accuracies can cause the two duties to be unequal. In general, the agreement between the two duties was very good. At flow rates higher than 2500 gpm duties were within 5% (Figure 3-8). At lower duties and low flow rates, the discrepancy between the two measured values is magnified, with the worst being 22% off.

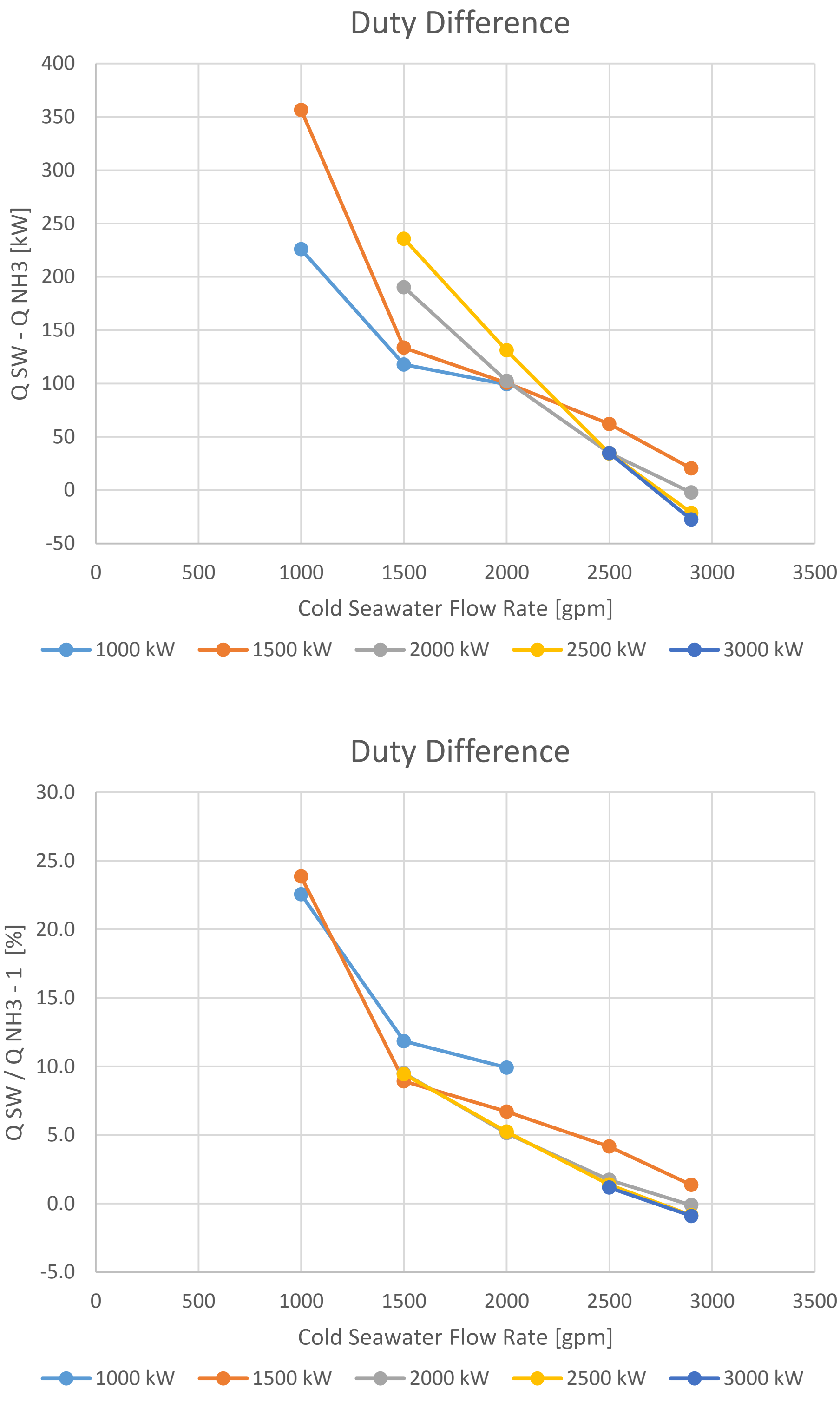

Figure 3-8. Difference between ammonia duty and seawater duty

3.1.8. Design Discussion

The APV Titanium Plate and Frame Heat Exchanger had high overall heat transfer coefficient but also high seawater pressure drop. The ammonia-side convection coefficient limits the overall heat transfer coefficient, so it may be possible to achieve comparable performance with lowered seawater pressure drop by lower resistance to flow on seawater channels.

3.2. APV TITANIUM CROSS FLOW PLATE-FRAME HEAT EXCHANGER

The APV Cross Flow Evaporator is titanium plate-frame type heat exchanger. This heat exchanger has a nominal thermal capacity of 2MW, like the previous five heat exchangers tested at OERC. The plate size and type are identical to those within the previously tested APV condenser. However, the shape of the corrugations are modified to optimize convection to increase boiling.

Similar to the previously tested APV titanium plate-frame condenser, the APV cross flow evaporator uses large plates which reduces the total number heat exchangers required, and thus the number of manifold pipes and flange connections that will be required in a large OTEC power plant. To further reduce manifold costs, Makai and APV designed a cross-flow evaporator that eliminates the need for seawater manifolds, leading to a 50% reduction in manifold costs. This new design required custom tooling to fabricate the plates. Seawater enters through the side and passes through horizontally. Furthermore, the design of the heat exchanger provides a more elegant mounting solution inside the Remora (the offshore superstructure which houses all power cycle components, including heat exchangers, tanks, water pumps, etc.), allowing for a reduction in the total size of the system.

Table 3-3. Evaporator Properties

Plate Properties	
Material	Titanium ASTM B265 Grade1
Number of Plates	149 total, 147 heat transfer
Plate Thickness	0.6 mm
Total heat transfer area	332.514 m^2 total, 277.8 m^2 effective

Frame Properties	
Material	Carbon Steel
Frame Height	3.24 m
Frame Width	1.73 m
Frame Length	1.73 m
Max Number of Plates Pairs	74 + 1 single

The APV cross-flow evaporator was installed and tested in October 2014. A total of 21 operating points were tested (Table 3-4). Each operating point was held at steady state for at least ten minutes. Steady state was defined as being within +/- 3% for duty, +/- 2% for seawater flow rate, +/- 0.1°C for seawater inlet temperature, +/-0.1°C for seawater temperature difference, and +/- 2% for LMTD.

Figure 3-9. APV Cross Flow Heat Exchanger installed at the OERC HX Performance Testing Facility.

Table 3-4. APV Cross Flow Evaporator Test Points Matrix

		Duty [kW]			
		1500	2000	2500	3000
Warm Water Flow (gpm)	1500	X	X		
	2000	X	X	X	
	2500	X	X	X	X
	3000	X	X	X	X
	3500	X	X	X	X
	4000	X	X	X	X

3.2.1. Overall heat transfer coefficient

U was mostly dependent on water velocity and less dependent on duty. This indicates that the heat exchanger is limited by the water-side heat transfer rate.

The effect of quality on U was not explicitly tested but two test points collected at different qualities illustrate U is lower for high qualities. The 4000 gpm – 2500 kW (green filled circle) operating point and one of the 4000 gpm – 3000 kW (red "x") operating points were collected at high quality (82% and 94%, respectively) compared to the other points at ~ 60 % quality. At 4000 gpm – 2500 kW, the U value at 82% quality is slightly lower than expected from the trend at ~60% quality; the slope of the gray dashed line is not as steep as the solid gray line. U value for the 94% quality point at 4000 gpm – 3000 kW is 2% lower than for the 60% quality point at 4000 gpm – 3000 kW. Previous testing indicated U is mostly independent of quality variations between 30-80% but decreases with increasing quality at qualities higher than 80%.

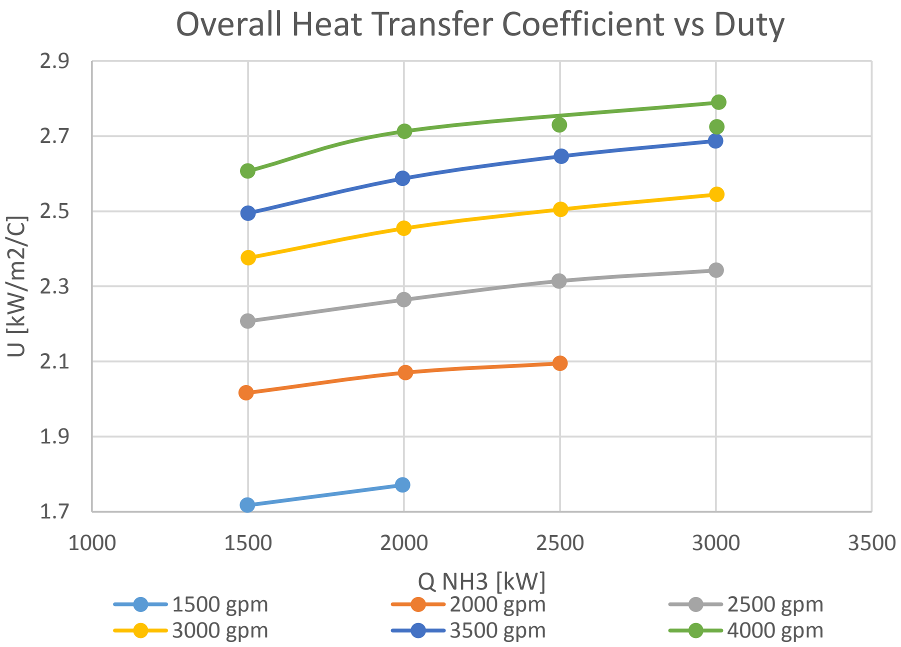

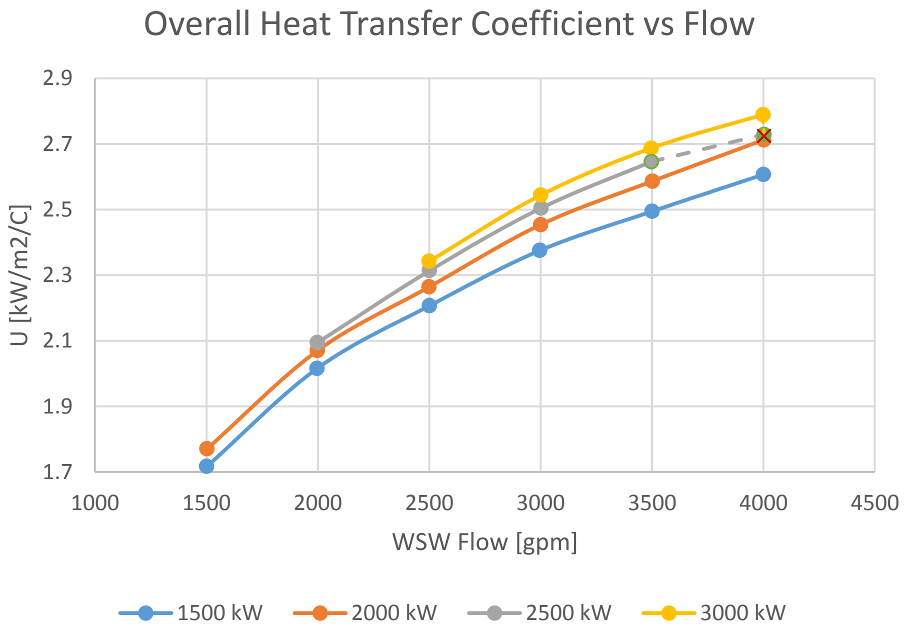

Figure 3-10. Overall heat transfer coefficient

3.2.2. Convective heat transfer coefficients

In the tested range, the overall heat transfer coefficient was mainly influenced by the seawater convective heat transfer coefficient which varied from 3.5 to 11 kW/m^2-C whereas the ammonia convective heat transfer coefficient showed little change (3.8 to 4.3 kW/m^2-C).

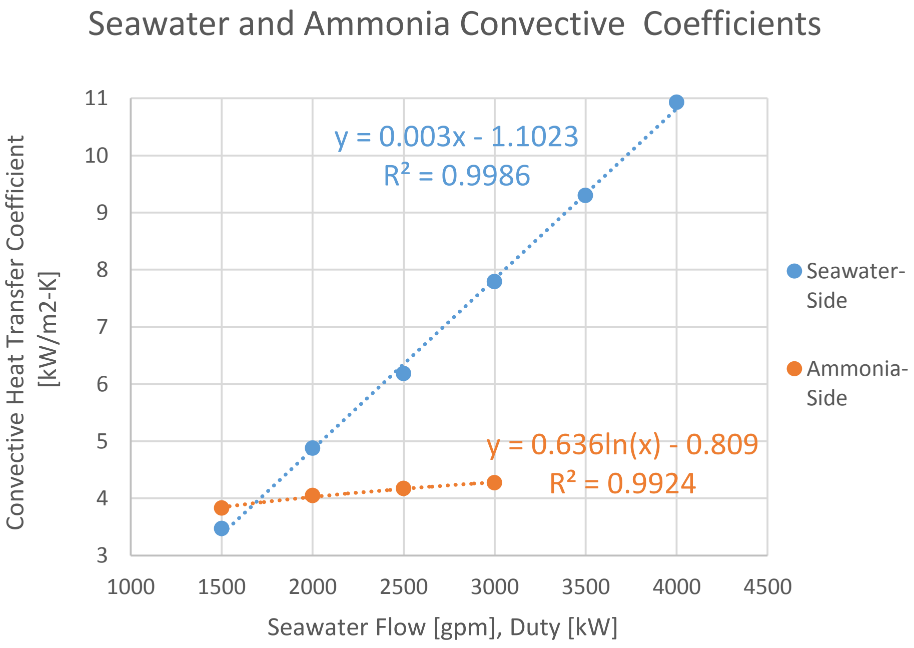

Figure 3-11. Ammonia and seawater convective heat transfer coefficients fitting the equation $1/U = 1/h_{sw} + dx_w/k + 1/h_{NH3}$ solved for using the least–squares method.

3.2.3. Seawater-side pressure drop

The seawater-side pressure drop is independent of duty and has a power-law relationship to flow rate with an exponent of ~1.9. However, with less than 10 kPa pressure drop at 4000 gpm, the pumping power requirement is quite low.

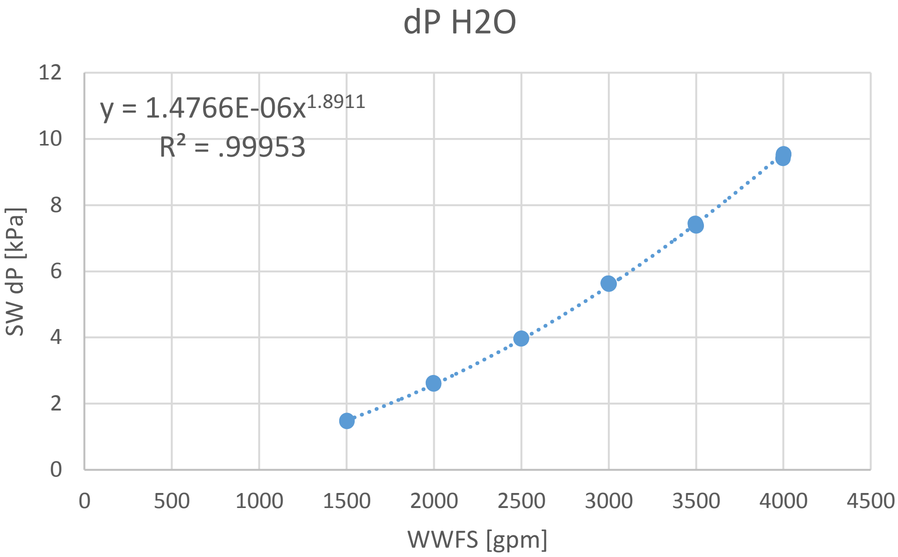

Figure 3-12. Seawater-side pressure drop

3.2.4. Ammonia-side pressure drop

Ammonia-side pressure drop is independent of seawater flow, increases with increasing duty, and decreases with increasing quality because it is dependent on ammonia mass flow rate (Figure 3-13). The black triangles are points collected at high quality (82% and 94%).

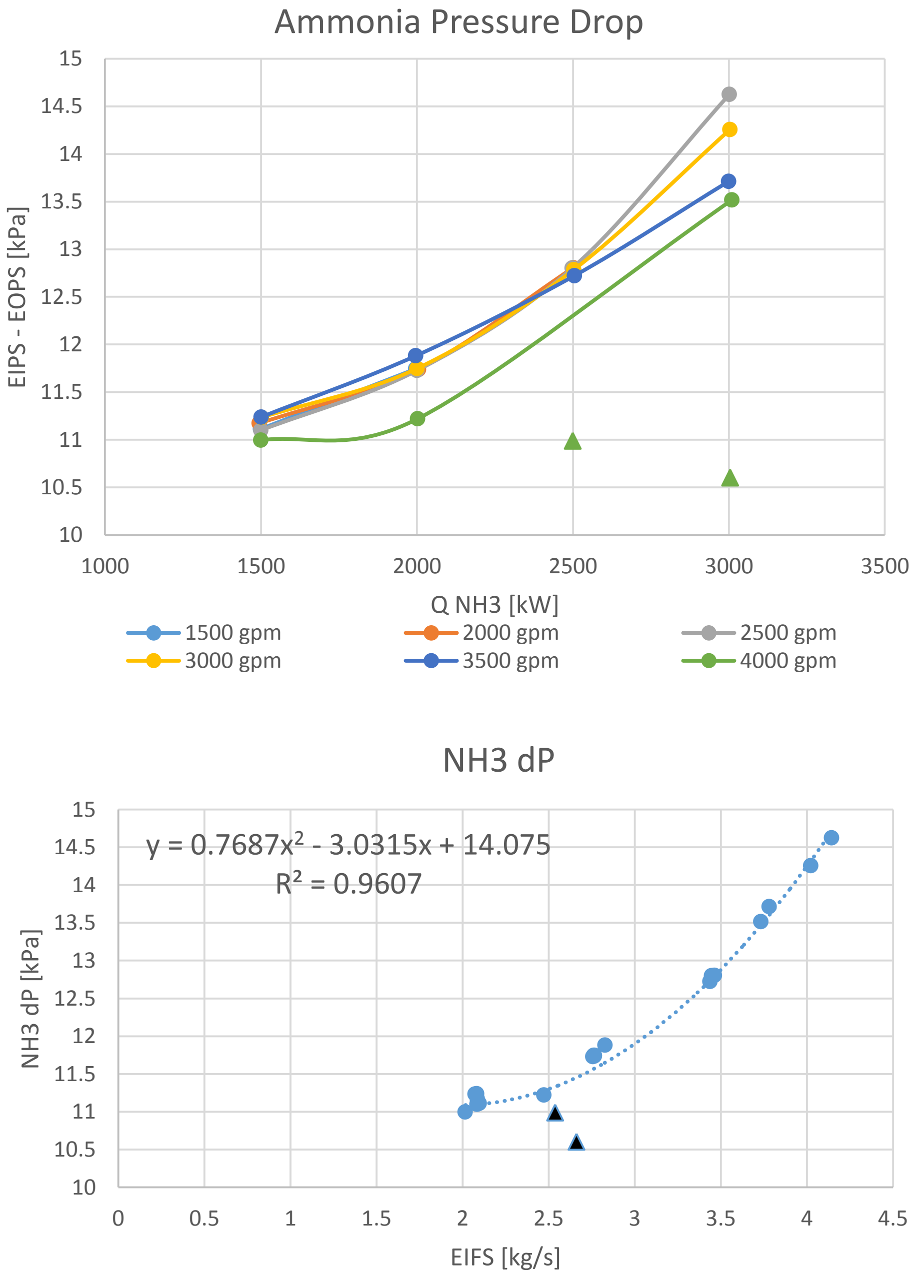

Figure 3-13. Ammonia-side pressure drop. Triangle data points were collected at higher quality than the other points. Since quality effects were not specifically tested, the high quality points are considered outliers, shown for completeness but not included in analysis.

As measured, ammonia-side pressure drop is 5 times higher than the predicted but the as-measured pressure drop also includes the effects of static head and momentum head along with frictional head loss. By solving for the void fraction at different heights along the evaporator, the static head and momentum head contribution to the total pressure drop can be calculated, leaving the only the pressure drop due to frictional losses (Figure 3-14).

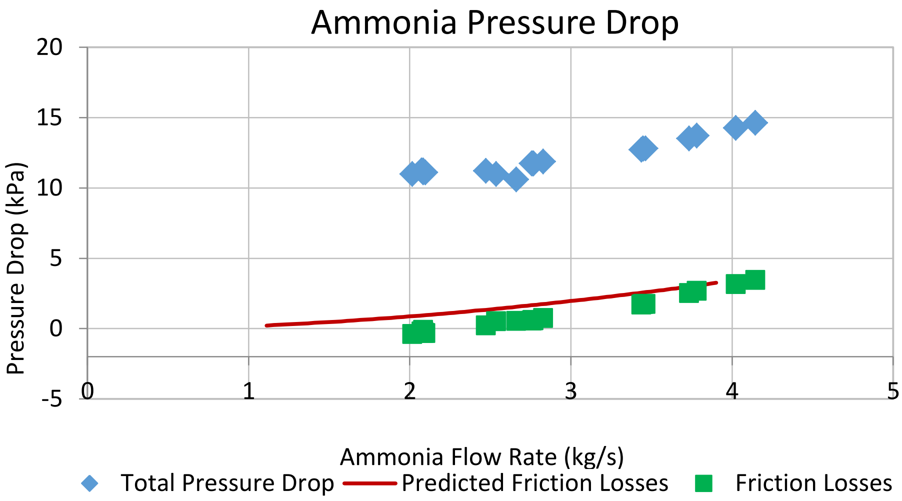

Figure 3-14. Ammonia-side frictional losses.

3.2.5. Ammonia-side operating pressure

For a given duty, the evaporator pressure increases with increasing seawater flow. This means that gross power is greater for higher seawater flow rates; however, seawater pressure drop increases exponentially with increasing seawater flow which increases pumping power and ultimately reduces net power. As with the overall heat transfer coefficient, there is an optimum point which maximizes the gain in power output with increased seawater flow while accounting for the increase in pumping power required at higher seawater flow rates to produce the maximum net power.

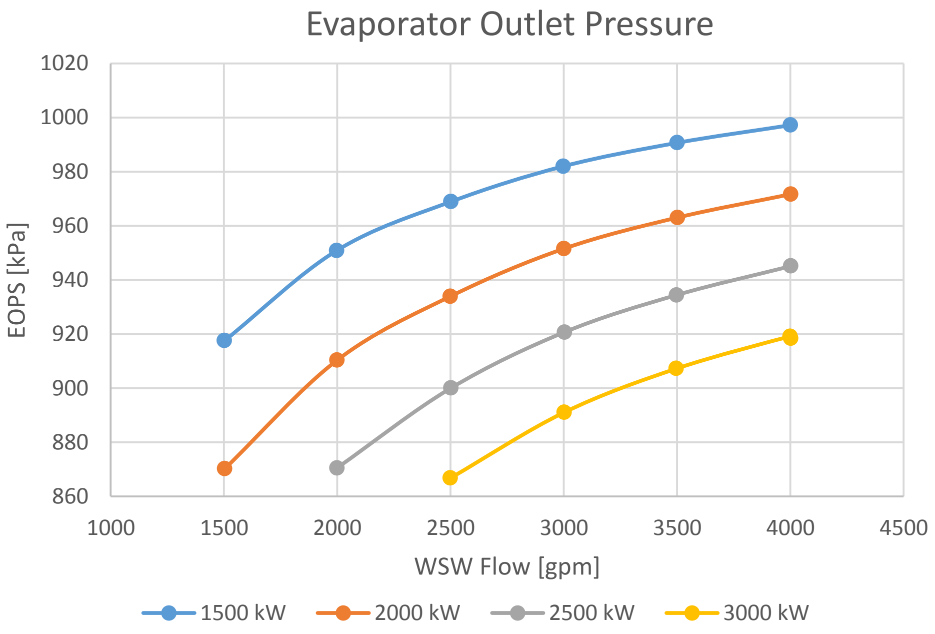

Figure 3-15. Ammonia absolute pressure at evaporator outlet increases with increasing seawater flow rates.

3.2.6. Difference between ammonia and seawater duty

Theoretically, if the evaporator was perfectly insulated, the ammonia duty should be identical to the seawater duty. However, environmental input and limitations in sensor accuracy can cause the two duties to be unequal. The two duties were within 6% (Figure 3-16). Previous testing showed greater duty discrepancy at lower flow rates and lower duties. Duty discrepancy is greater at lower duties but contrary to previous testing, higher flow rates also resulted in higher discrepancies for the same duty.

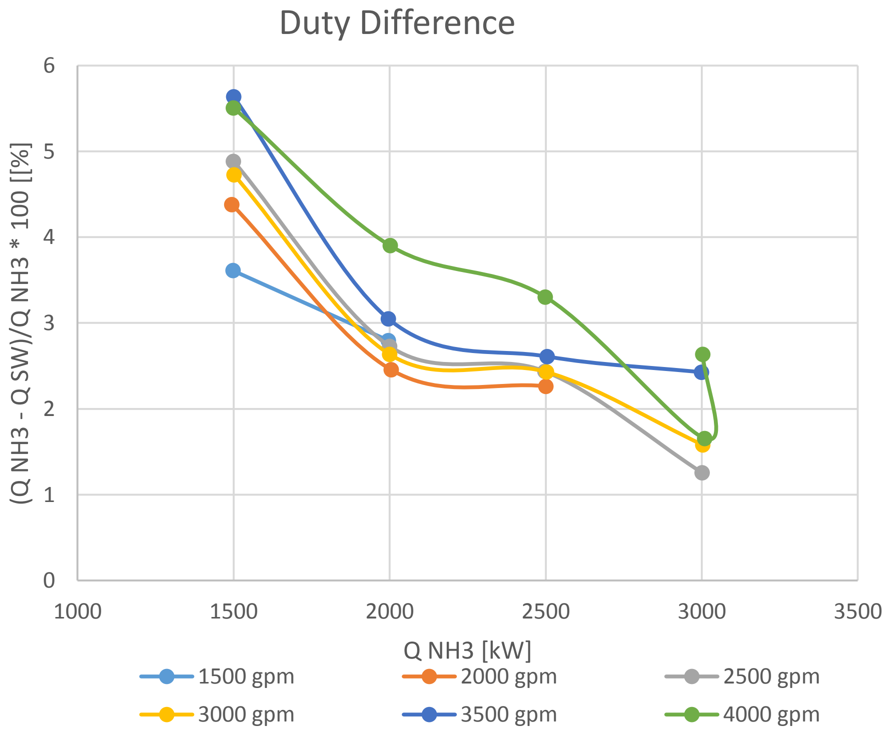

Figure 3-16. Difference between ammonia duty and seawater duty

3.2.7. Approach Temperature

The data shows a linear relationship between duty and approach temperature, with the slope of the line dependent on the water velocity. The approach temperature increases with duty because higher duty corresponds to higher ammonia operating pressure, and thus a higher saturation temperature.

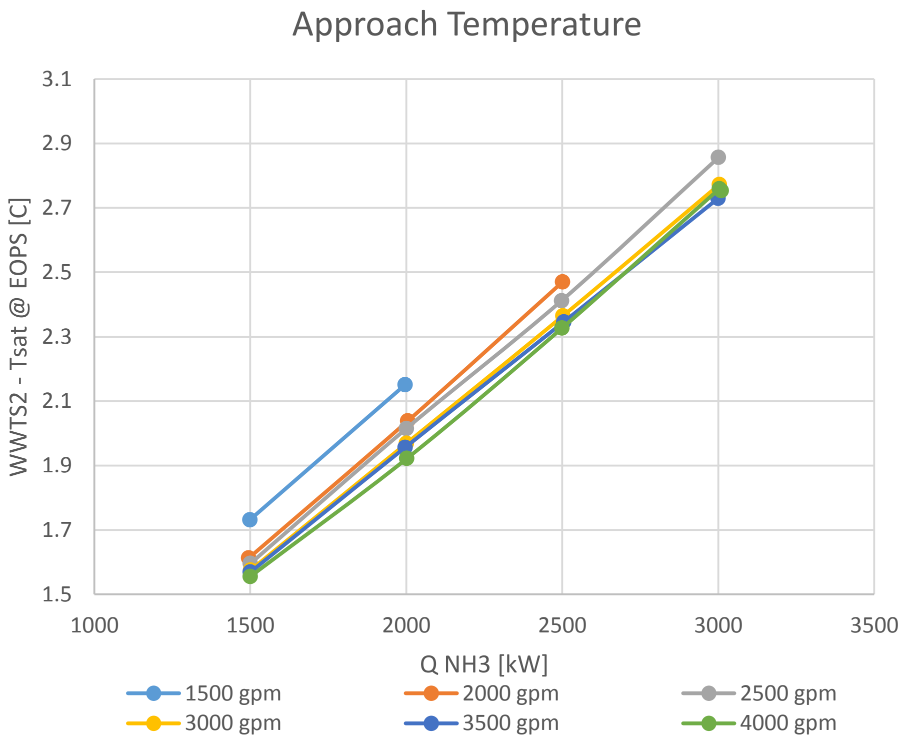

Figure 3-17. Approach temperature

3.2.8. Design Discussion

Similar to the APV condenser, the ammonia-side convection coefficient limited the overall heat transfer coefficient. For the cross-flow evaporator, seawater pressure drop was very low so higher flow rates could be used. Design adjustments to enhance ammonia-side convection could improve the evaporator performance. As tested, the APV Cross Flow evaporator performance was average but likely need improvements for an OTEC heat exchanger.

3.3. LOCKHEED MARTIN HORIZONTAL EVAPORATOR

The Lockheed Martin Horizontal Evaporator was installed and tested in October 2014. 34 operating points were tested, some points were tested with variations in quality, evaporator level, and pre-heating. Makai gained insight into the operation of a horizontal evaporator and differences in performance of horizontally versus vertically oriented heat exchangers.

4. CORROSION TESTING

Makai Ocean Engineering, Inc. has been conducting corrosion testing in support of OTEC heat exchanger design at OERC since 2009. Potential heat exchanger materials and fabrication methods are tested in conditions representative of OTEC operations. Aluminum alloys, which were selected for their cost-effectiveness and variety of fabrication options, have been extensively tested. Samples tested at the OERC are exposed to seawater representative of OTEC operating conditions (warm surface seawater (WSW), cold seawater (CWS) from ~674 m, and deep seawater (DSW) from ~915 m).

Uniform general corrosion rates for aluminum alloys are acceptable but localized corrosion (pitting and crevice corrosion), particularly in CSW, is of concern. Aluminum alloys have performed well in WSW and show promise for use in an evaporator. In particular, Alloy 3003 has performed the best in WSW. Alloy performance has differed between the cold seawater sourced from 674-m and 915-m. In 674-m CSW, Alloys 3003 and LA83I have performed the best, but certain samples of each alloy had deep pits. In 915-m CSW, all alloys have severe pits. Alloy 3003 has performed the best, but still had a ~ 0.5 mm deep pit after four years of exposure.

After the first year of corrosion testing, Makai determined the established analytical methods were inadequate for OTEC purposes and began to develop new techniques to evaluate corrosion performance. Results from early tests also revealed poor performance of some samples and has prompted Makai to investigate treatments that could improve corrosion resistance. Makai developed instrumentation (daily, automated, high resolution imaging; in situ ultrasonic pit detection; and laser profilometry) to quantify the extent and severity of pitting. Makai has also been investigating treatments (curing in WSW, ozone flushing, and acid flushing) and coatings to prevent and/or mitigate the development of localized corrosion. Finally, Makai also evaluated biofouling controls.

4.1. BOX COUPONS

Box coupons have been tested since 2009. Four-year samples were removed in January 2014. All alloys are performing well in WSW, with little to no pitting. Pits are prevalent in Alloy 1100 and 6063 samples exposed to 674-m CSW and 915-m seawater. Alloys 3003, 5052, LA83I, and LA83P showed little pitting in 674-m CSW but all four alloys had significant pitting in 915-m CSW. Samples moved from surface seawater to 674-m CSW after 40 days have begun to show increasing pits.

Several changes have been made to the reporting of pitting data. The maximum pitting depth is reported in place of the average of the maximum pit depths for all the samples of each alloy in each water source. Since a single failure in a heat exchangers constitutes failure of the heat exchanger, the maximum for all samples of the same alloy in each water source is now reported.

To capture the extent of pitting, each scanned surface was divided into 0.5 x 0.5 mm squares. The maximum pitted depth in each 0.5 x 0.5 mm square was recorded and the results were plotted in histogram form for each sample. Samples of the same alloy in the same water were also combined into one histogram for overall alloy performance per water source, over time.

Corrosion product buildup can reduce heat exchanger performance. Since heat exchanger performance is function of the available heat transfer surface and measured for the entire heat exchanger, the average pitted area, as a percentage of total area, is reported. However, corrosion product accumulates beyond the residual pitted area (up to several times the pitted area); therefore, the actual heat transfer area that is affected by corrosion will be greater than the average pitted area. The relationship between pitted area and corrosion buildup area varies between the different alloys and warrants further investigation.

4.1.1. WSW

Table 4.1-1 summarizes the number of sample scanned per alloy, per exposure time. For samples removed at the earlier exposure times, not all samples that were removed were scanned.

Table 4.1-1. Number of scanned WSW samples.

	1yr	1.5yr	21mo	2yr	3 year	4 year
1100	-	2	-	4	2	4
3003	-	2	-	4	2	4
5052	-	3[a]	-	4	2	4
6063	1	2	-	4	2	4
LA83I	-	2	-	4	2	4
LA83P	-	2	-	4	2	4

[a] 3 of 4 samples were scanned, scan quality was poor on 1 of the 3 scanned samples; data from poor scan not shown in figures or used in analysis.

For the four-year samples, profilometer scans identified one pit each on two samples (one of Alloy 1100 and one of Alloy LA83I, Figure 4-1) although the pits could not be visually identified under a microscope. No pits were observed on the remaining 22 samples.

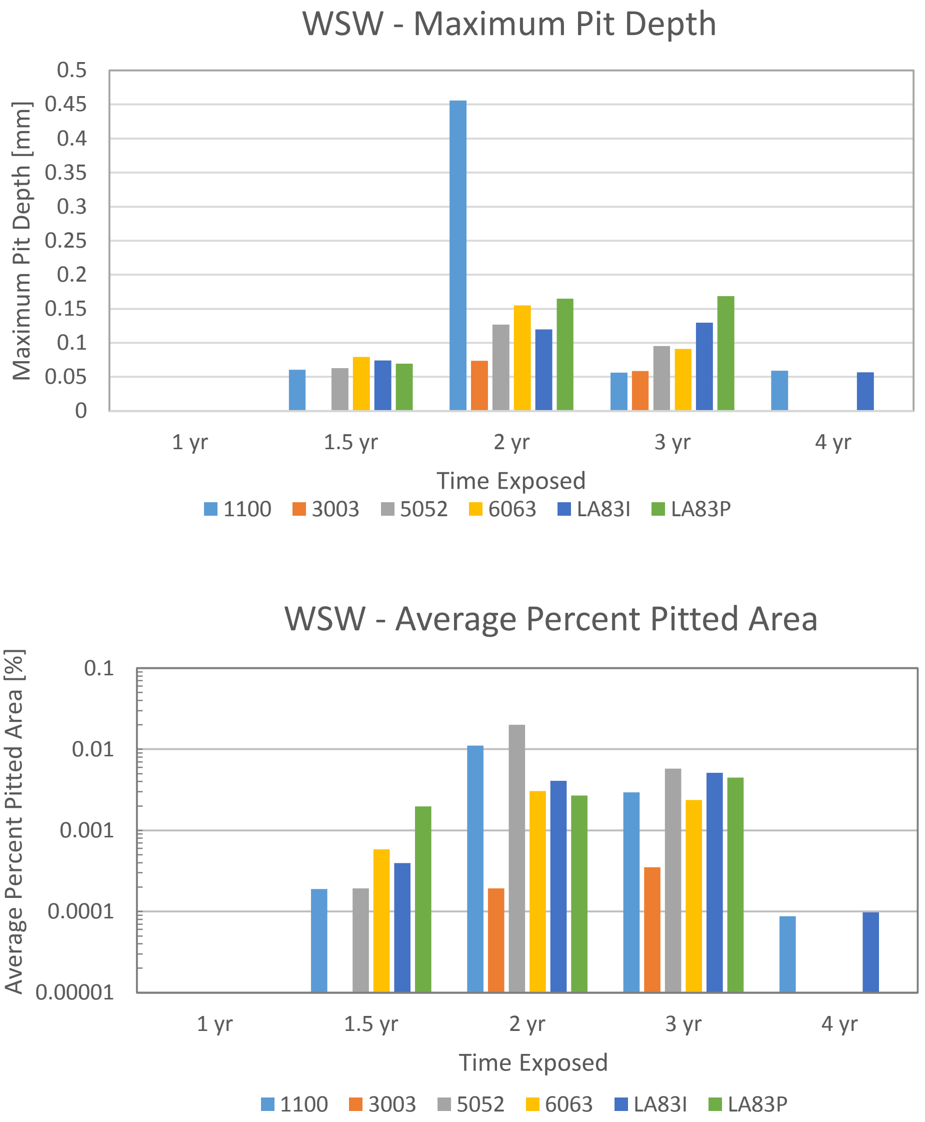

Figure 4-1. Maximum pit depth and average percent pitted area (per alloy, per exposure time) for samples exposed to WSW. There are no scan data for 1-yr exposure samples of Alloys 1100, 3003, 5052, LA83I and LA83P.

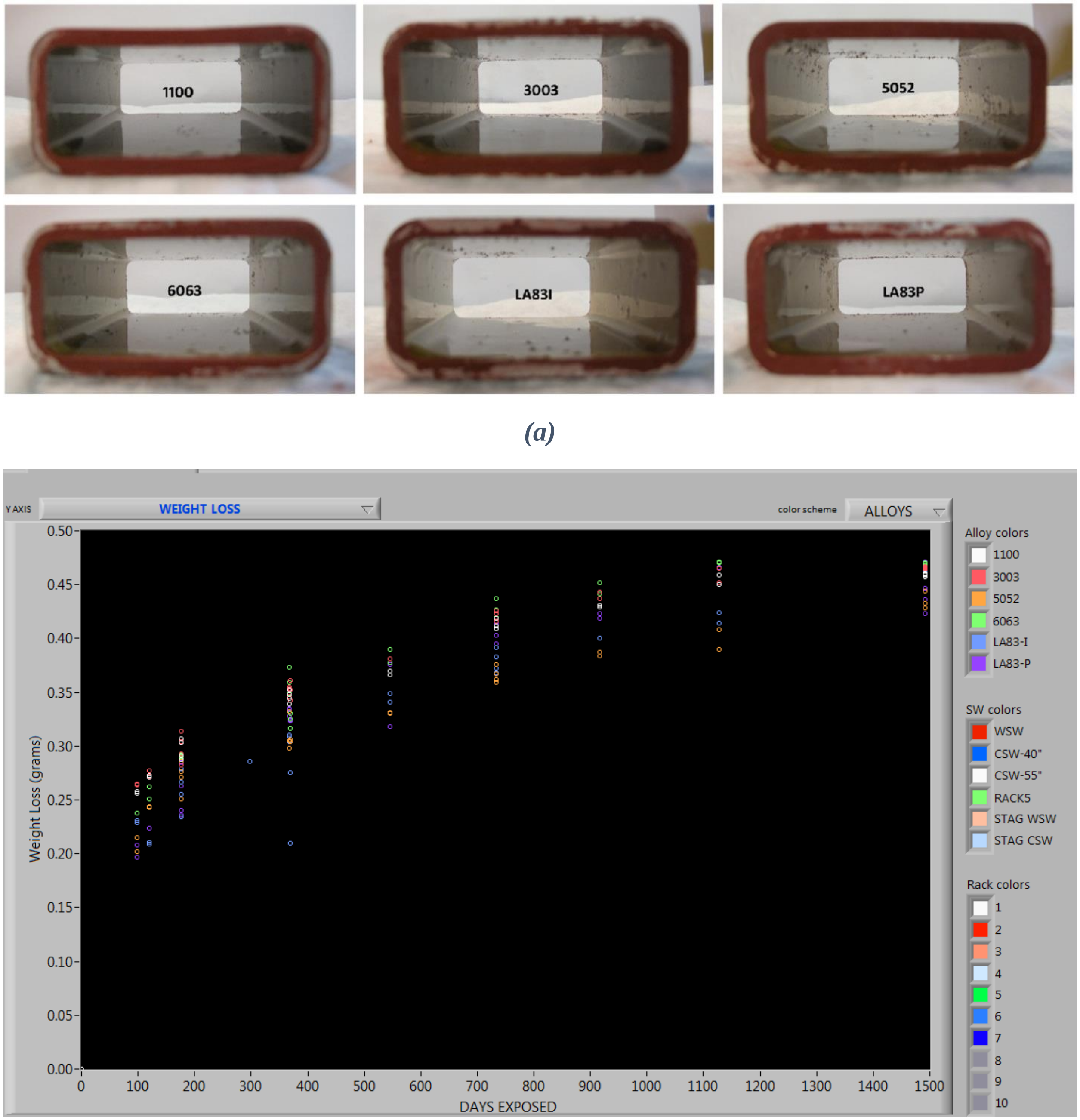

(a)

(b)

Figure 4-2. (a) Representative images and (b) weight loss results of samples exposed in WSW for four years.

All alloys continue to perform well in WSW. The four-year samples had less pitting than the three-year samples. Weight loss results also indicate the four-year samples were performing better than the three-year samples. This trend will have to be evaluated when the five-year samples are analyzed.

4.1.2. Cold Seawater (CSW)

For Alloys 1100 and 6063, pitting was severe. Both samples of Alloy 6063 had deep extrusion defects which have been observed to be either pit initiation sites or sites more susceptible to pitting. Both Alloy 1100 samples exhibited crevice corrosion. One sample even had severe corrosion on the exterior surface, likely caused by leakage stemming from crevice corrosion.

Table 4.1-2 summarizes the number of sample scanned per alloy, per exposure time. Not all the 1-yr and 21-month samples that were removed were scanned.

Table 4.1-2. Number of scanned CSW samples/total removed samples.

	1yr	1.5yr	21mo	2yr	3 year	4 year
1100	4	4	-	4	2	2
3003	-	4	-	4	1	2
5052	-	4	8	4	2	2
6063	2	4	9	4	2	2
LA83I	-	4	-	4	2	2
LA83P	-	4	1	4	2	2

One CSW rack was inspected at 21 months due to excessive leaking. Three samples of LA83I were removed and visually inspected to have pits but were not scanned by the profilometer. An additional three pitted samples of Alloy 6063 were removed after 21 months but not scanned (12 samples removed total). Crevice corrosion induced leaks likely contributed to further worsening of crevice corrosion and pit development. Since samples were visually inspected and the worst samples were removed, the data are biased.

For the 4-yr samples, some discrepancies between the profilometer analysis and microscope inspection were identified. Pits identified on LA83I-35 correspond to a relatively large area where the sample surface appears gouged (Figure 4-3). Profilometer scans cannot distinguish between scratches or other pre-existing surface defects and pits. Some variability is expected due to surface imperfections. For both Alloy 5052 samples, profilometer scans identified several shallow pits but visual inspection identified one pit on one Alloy 5052 sample and no pits on the other sample. With Alloys 3003 and LA83P, pits identified on profilometer scans were also not identified visually. Rescanning the samples did not resolve the discrepancy; however, since the maximum pit depth for all four alloys was ~ 0.1 mm, it is more likely the pits were not discernible under the microscope or some surface features biased the algorithm for pit identification. Pitting was not severe in the four-year samples of Alloys 3003, 5052, LA83I, and LA83P.

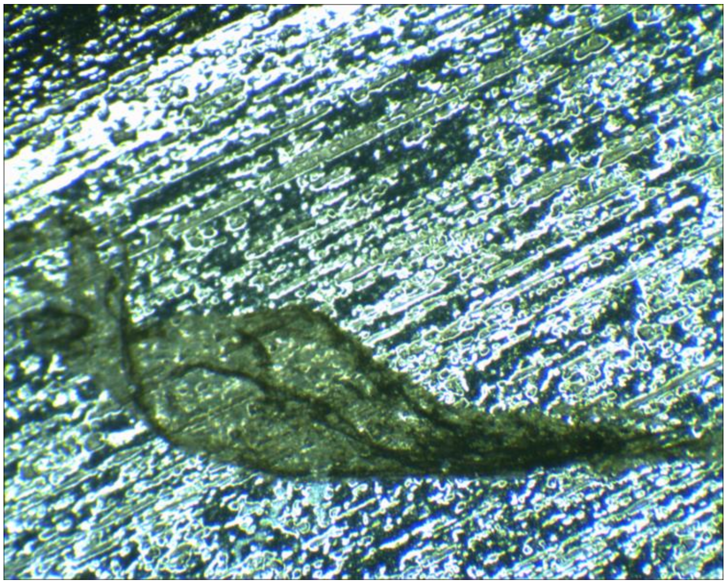

Figure 4-3. Pitted area identified in profilometer scan on LA83I-35. Under microscope inspection, the area does not display characteristics of pitting, rather the surface appears gouged or eroded.

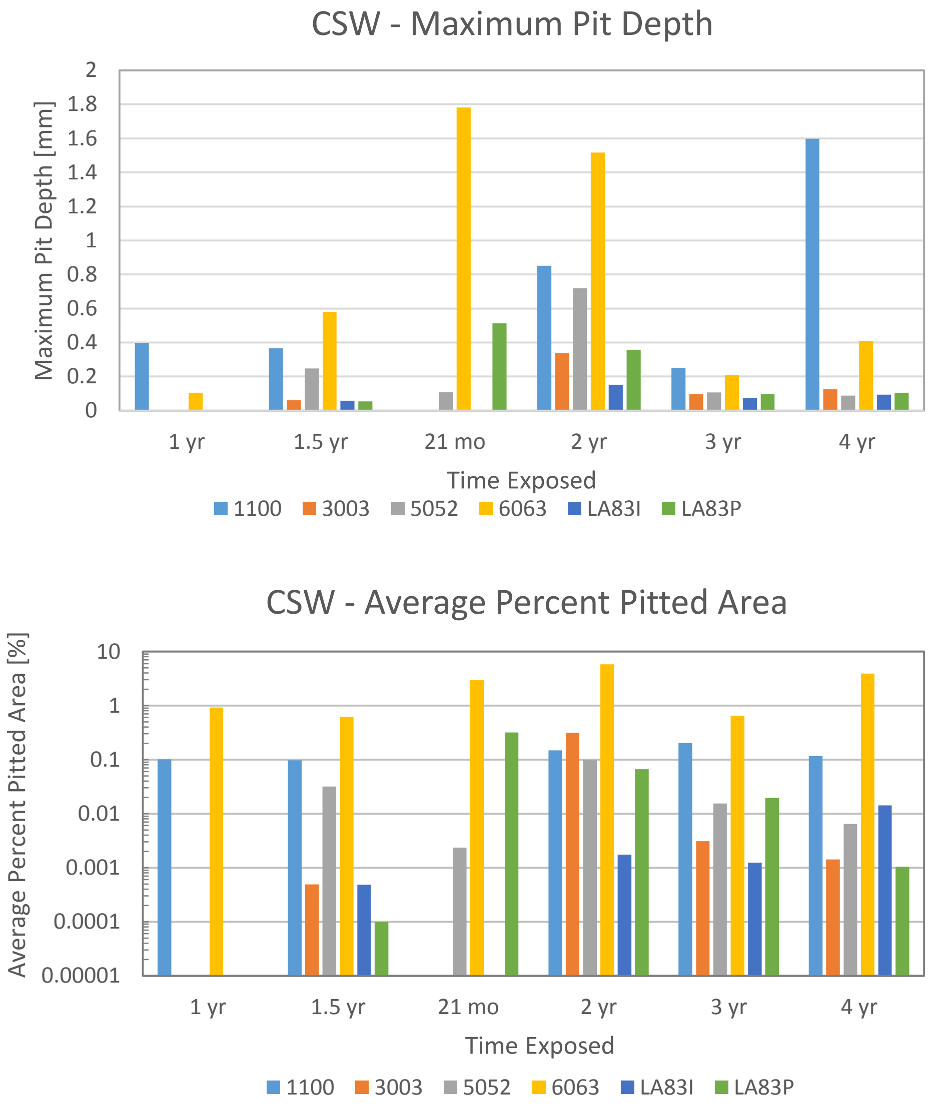

Figure 4-4. Maximum pit depth and average percent pitted area (per alloy, per exposure time) for samples exposed to CSW. There are no scan data for 1-yr exposure of Alloys 3003, 5052, LA83I, and LA83P and 21-month exposure of Alloys 1100, 3003, and LA83I.

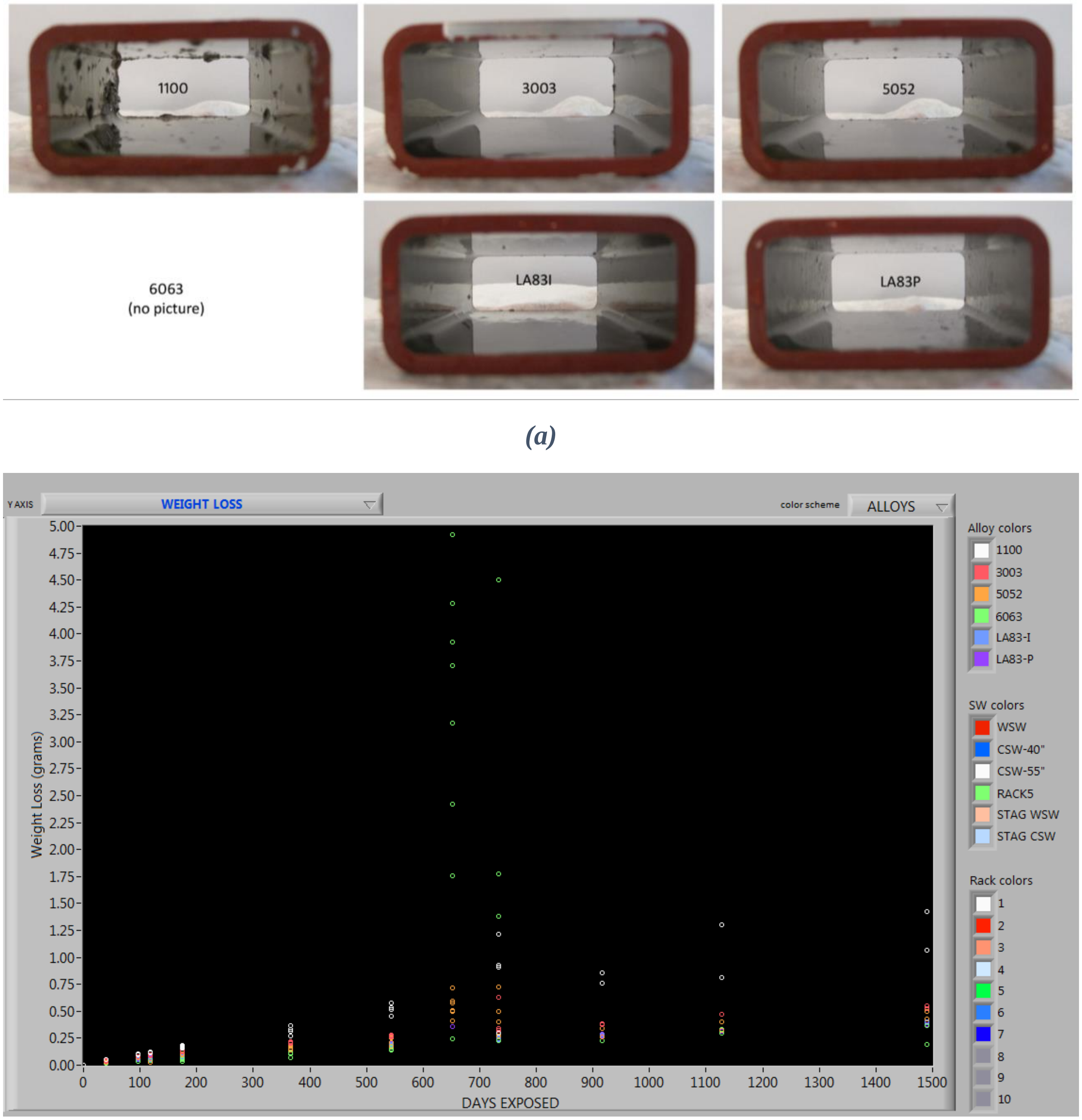

(a)

(b)

Figure 4-5. (a) Representative images and (b) weight loss results of samples exposed in CSW for four years.

There are some anomalies in weight loss results for the 21 month and 2 year samples. Alloys 5052 and 6063 had lower three- and four-year weight loss than 21-month and two-year weight loss. 21-month the 2-year data were obtained from samples in different CSW racks but severe crevice corrosion was noted in Alloy 5052 and 6063 samples for both exposure times.

4.1.3. Deep Seawater (DSW)

All alloys performed poorly in DSW. In addition to pitting corrosion, crevice corrosion was also severe. Table 4.1-3 summarizes the number of sample scanned per alloy, per exposure time. Although 1 year samples of all alloys were removed, only Alloy 1100 samples were scanned.

Table 4.1-3. Number of scanned Deep Seawater (DSW) samples.

	1yr	1.5yr	21mo	2yr	3 year	4 year
1100	6	1	-	3	2	2
3003	-	1	-	4	2	2
5052	-	1	-	4	2	2
6063	-	1	-	4	2	2
LA83I	-	1	-	4	2	2
LA83P	-	1	-	4	2	2

Compared to other water sources, pitting and crevice corrosion was worst in DSW; nearly all samples had pits and crevice corrosion. Several samples were so severely corroded that corrosion product removal was incomplete; the actual maximum pit depth and pitted area is higher than that recorded by the profilometer. Useful profilometer scans are limited to the flat coupon surfaces, away from sides and edges; hence the extent of crevice corrosion is not entirely captured by a scan and visual observations are required.

Both LA83P samples also had large pits on the sides of the samples which could not be scanned by the profilometer.

Figure 4-6. One of several large pits on LA83P samples in DSW. These pits are located along the sides of the sample and cannot be scanned by the profilometer.

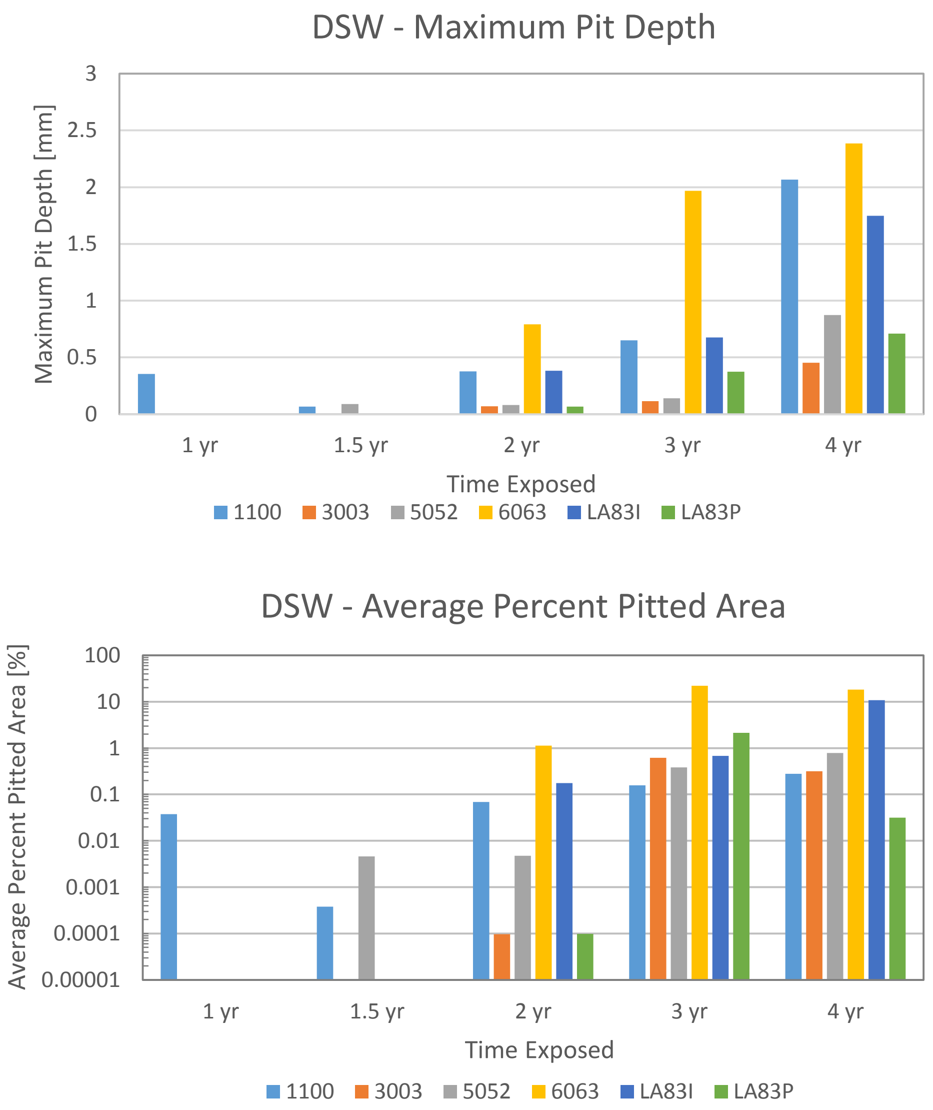

Figure 4-7. Maximum pit depth and average percent pitted area (per alloy, per exposure time) for samples exposed to DSW. Pits were prevalent on DSW samples. Only Alloy 1100 1-year samples were scanned. No profilometer data is reported for the 1-year samples of the other alloys. (No pits were observed, only two of Alloy 5052 samples had small blisters but no pit craters). Many of the 4-year samples had pits on the edges and sides of the coupon that could not be captured in the profilometer scans.

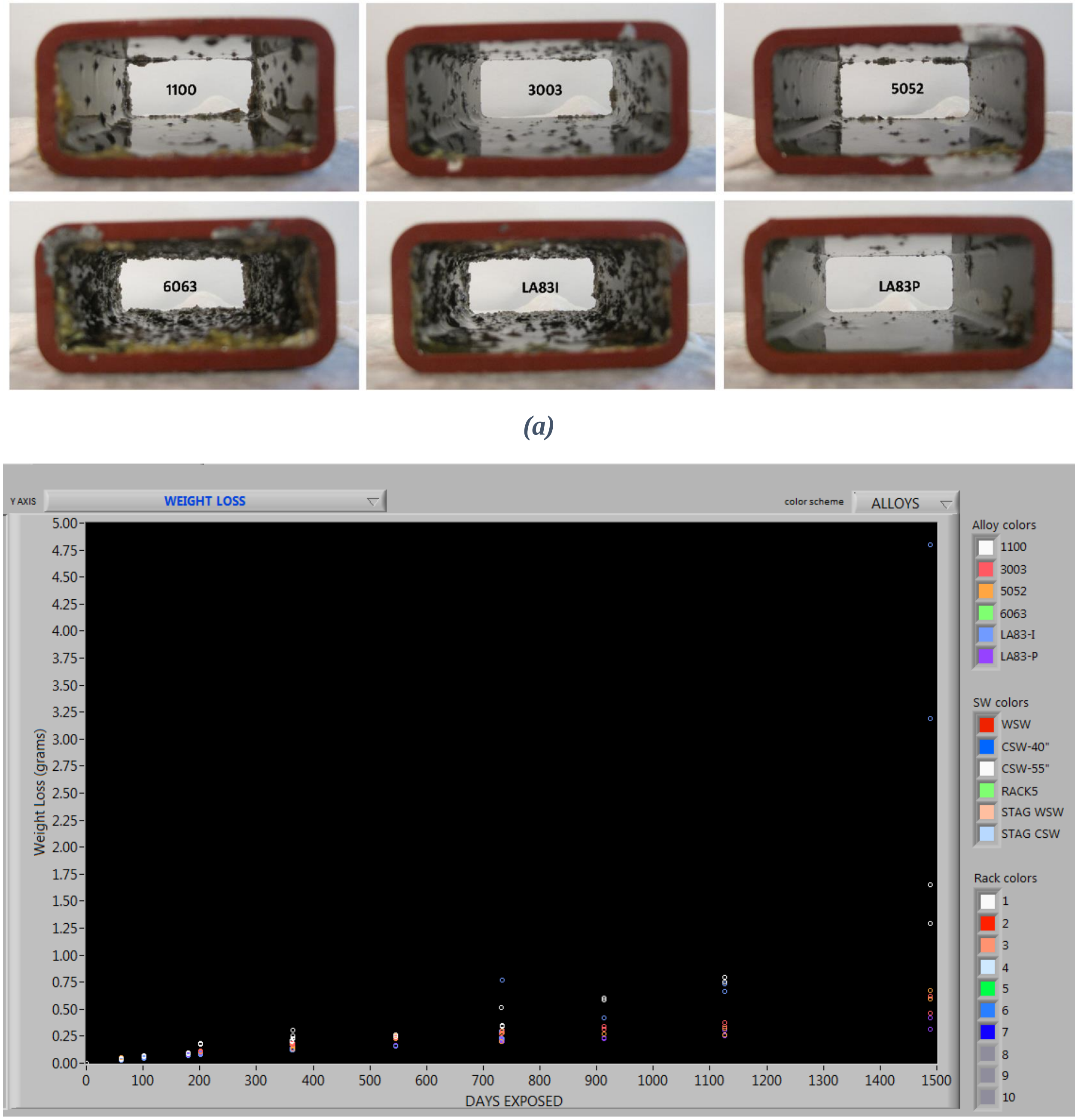

(a)

(b)

Figure 4-8. (a) Representative images and (b) weight loss results of samples exposed in DSW for four years. Results for Alloy 6063 are not shown. Alloy 6063 exhibited severe pitting along extrusion lines. Both samples removed after four years exposure had weight loss over 9.5 grams.

4.1.4. Warm Seawater (WSW) Pre-Treatment

In general, pitting was not severe in the WSW pre-treated samples. Table 4.1-4 summarizes the number of sample scanned per alloy, per exposure time. Although 1-year samples of Alloy 3003, LA83I, and LA83P samples were removed, they were not scanned with the profilometer.

Table 4.1-4. Number of scanned warm seawater (WSW) pre-treated samples.

	1yr	1.5yr	21mo	2yr	3 year	4 year
1100	3	-	-	2	2	2
3003	-	-	-	2	2	2
5052	2	-	-	2	2	2
6063	1	-	-	2	2	2
LA83I	-	-	-	2	2	2
LA83P	-	-	-	2	2	2

Of the 4-year samples, Alloys 3003, LA83I, and LA83P had little to no pitting. One sample of Alloy 5052 had extrusion defects and many small pits were concentrated within the extrusion defect channel. The other Alloy 5052 sample did not have extrusion defects and no pits were found. Alloys 1100 and 6063 continue to perform poorly. The maximum pit depth data for Alloy 1100 and 6063 samples are inaccurate due to incomplete corrosion product removal. On Alloy 6063, the pits appeared large and shallow. Both samples of Alloy 1100 also had severe crevice corrosion.

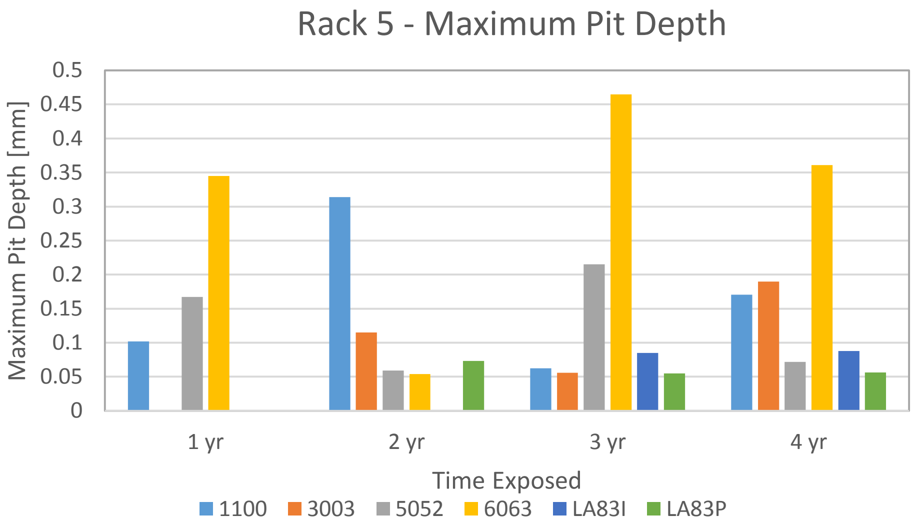

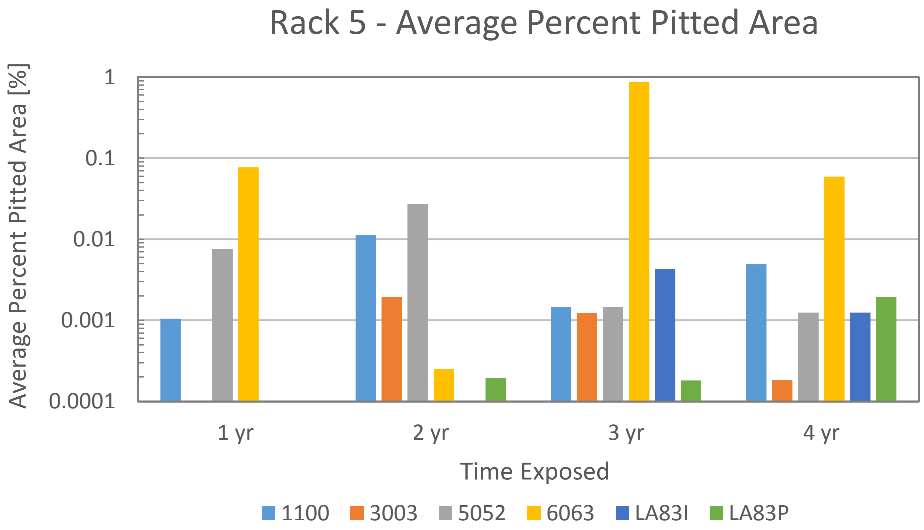

Figure 4-9. Maximum pit depth and average percent pitted area (per alloy, per exposure time) for WSW pre-treated samples exposed to CSW.

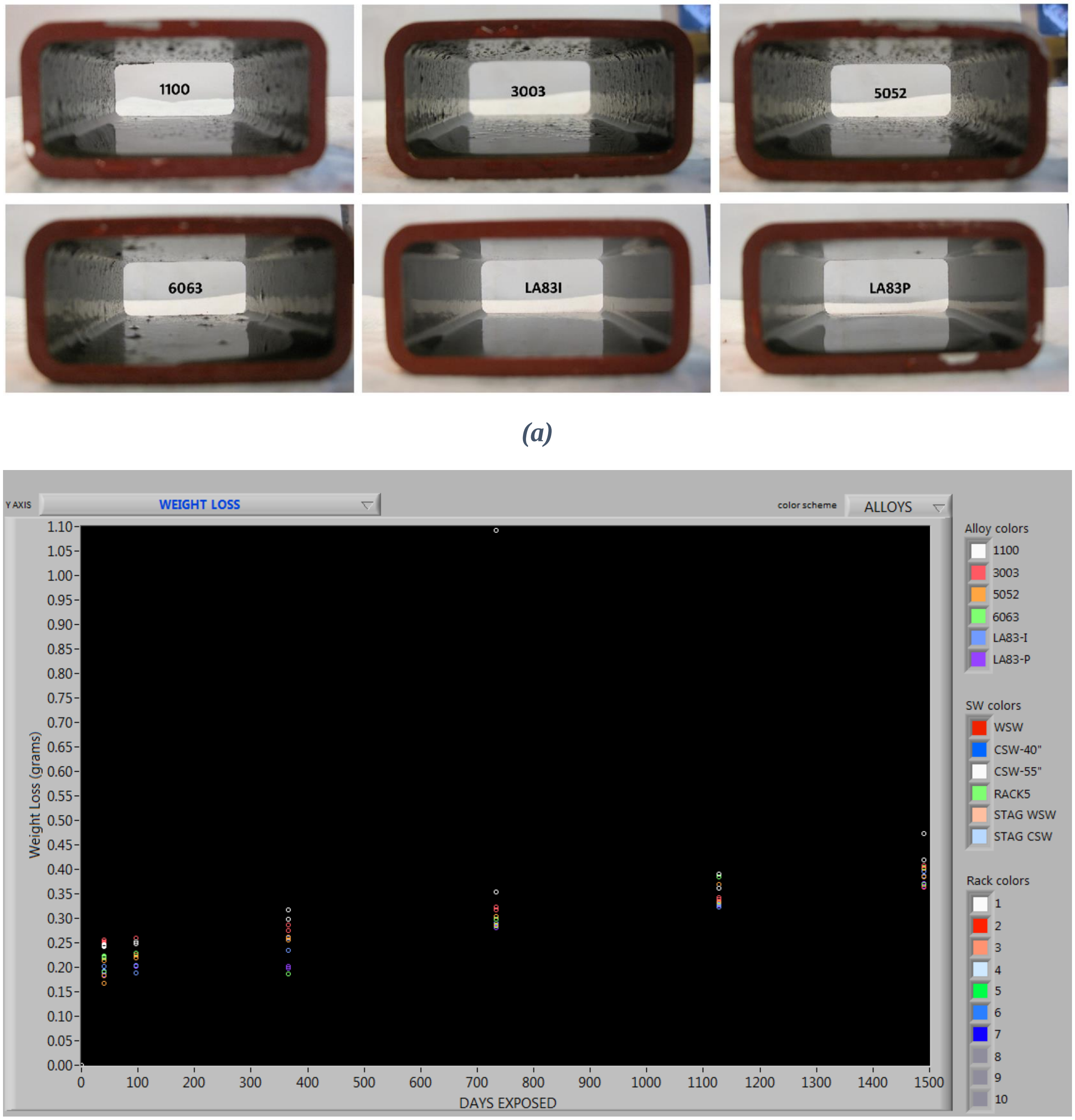

(a)

(b)

Figure 4-10. (a) Representative images and (b) weight loss results of samples exposed in WSW for 40 days, then moved to CSW for four years.

4.2. STEEL TUBE COUPONS

Recent images of the 674-m CSW intake during pipeline inspection showed galvanized steel hardware (installed during installation of the 674-m CSW pipe at NELHA ~ 30 years ago) in good condition, with the galvanized coating still intact. Makai decided to test galvanized steel as a possible material for the condenser.

Two sets of steel coupons, non-certified and certified have been exposed in CSW. Non-certified samples were exposed December 2012. Certified samples were exposed to CSW in June 2013. Coupons were weighed prior to exposure and monitored with electrochemistry. Two samples of each set were removed in January 2014 to provide 1 year (non-certified) and 6-month (certified) to provide for weight analysis. Electrochemistry was underestimating the corrosion rate.

Table 4.2-1. Corrosion rate of certified steel tube samples in CSW

	LPR Corrosion Rate [mpy]		**Weight Analysis Corrosion Rate [mpy]**
	1-day	3-month	6-month
CS7	0.308	0.208	N.A.
CS8	0.229	0.148	N.A.
CS9	0.136	0.096	2
CS10	0.121	0.084	2.2

Table 4.2-2. Corrosion rate of non-certified steel tube samples in CSW

	LPR Corrosion Rate [mpy]				**Weight Analysis Corrosion Rate [mpy]**
	28-days	35-days	6-months	9-months	1 year
Upper	0.116	0.177	0.081	0.166	1.9
Lower	0.207	0.176	0.142	0.089	1.8

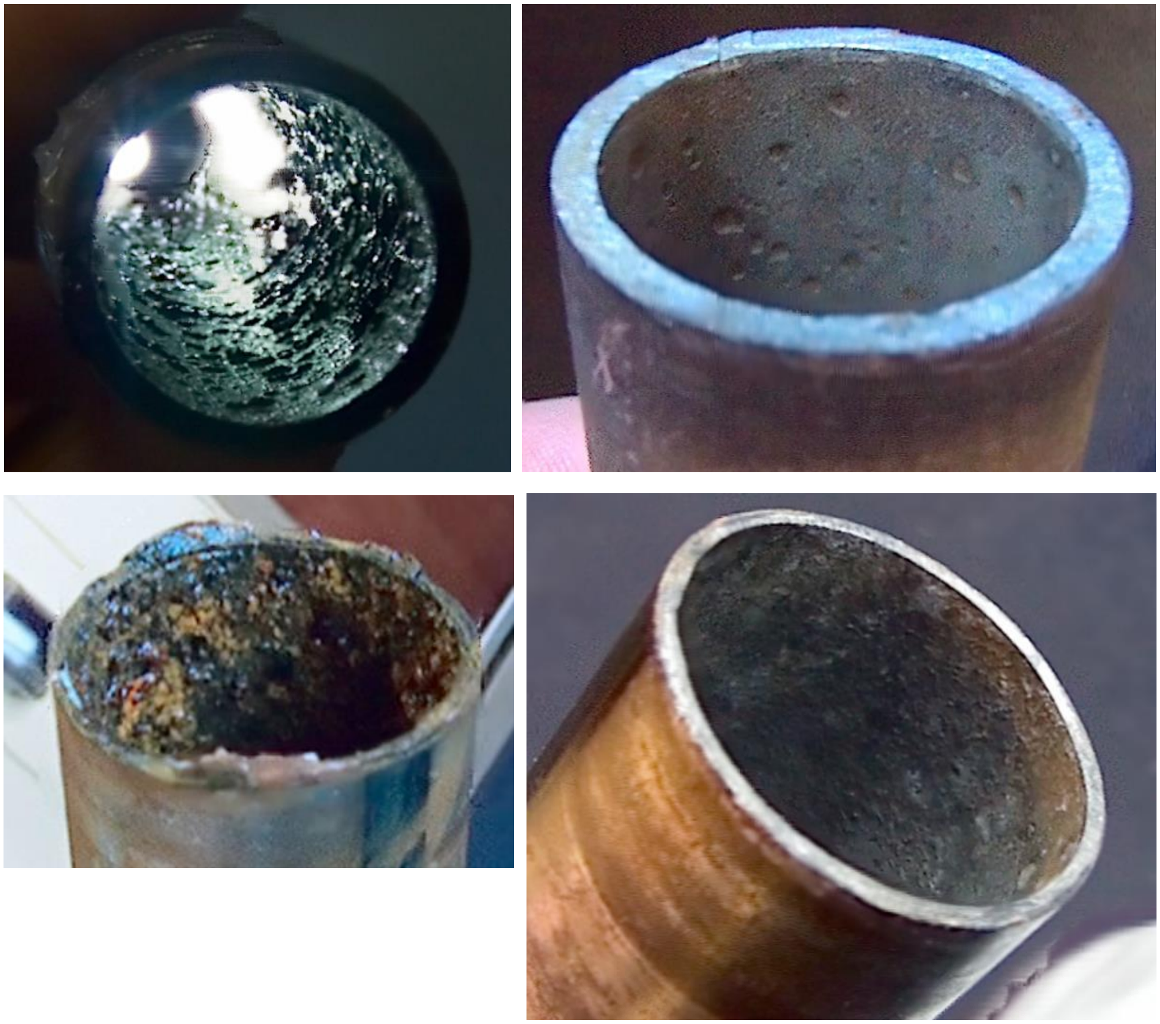

Figure 4-11. Certified steel sample after six months in CSW post-removal (top left) and post-processing (top right). Non-certified steel sample after one year in CSW post-removal (bottom left) and post-processing (bottom right). Post-processing reveals a relatively smooth wall with large shallow pits in the certified steel sample and a rough wall with few visible pits in the non-certified steel sample.

The inner surfaces of both types of tubes were roughened by corrosion product. Some corrosion product also began to flake off. Post-processing revealed certified steel samples still had relatively smooth walls that were covered with large shallow pits. The non-certified samples did not have large shallow pits, but the wall surface was no longer smooth.

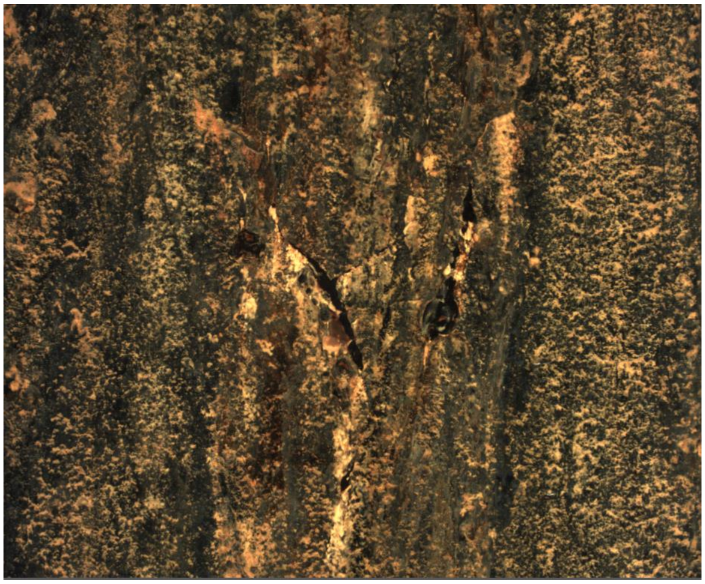

Figure 4-12. Corrosion product beginning to flake on a steel sample tested in the CSW MCIR.

Since the materials cost comprises about 40% of the total heat exchanger cost, a steel shell-and-tube condenser would provide ~10% cost savings over a similar aluminum condenser. However, the roughened surfaces will increase headloss (i.e., increased pumping power will be required) and the flakes of corrosion product will reduce heat transfer. The lowered performance of a steel condenser would not justify the relatively small cost savings and this test was discontinued.

4.3. ACID TREATMENT

Acid treatments are being investigated for their ability to clean the metal surface of impurities and to remove accumulated corrosion product. Nitric acid was first selected for testing but was found to be too aggressive for aluminum. Nitric acid preferentially attacked intermetallic compounds, which created pit initiation sites. Currently, sulfamic acid and citric acid are being tested. Acid concentration, treatment time, and treatment interval are under investigation. In addition to a set interval, e.g., every two months, Makai is also treating samples based on observation of OCP.

The acid treatment system consists of a storage/mixing tank and a series of valves and piping to deliver treatment to a specific sample. The acid treatment is flushed through a systems testing column for several minutes prior to sample exposure to ensure uniform application. Acid treatment lines are flushed with freshwater after treatment. Acid treatment is available for samples in the MCIR. Acid is recirculated through the sample column for two or five minutes per treatment. For samples with OCP-based intervals, the sample will be treated when OCP rises above -800 mV. This value is based on previously observed pitting when OCP reaches ~ -700 mV. The tests show that acid treatments can lower OCP to ~ -1000 mV for weeks to months before the OCP climbs again to ~700 mV.

Table 4.3-1. Current acid treatment samples in CSW.

Sample	Exposure Date	Acid	Interval	# of Treaments
AL 6063-T52	*9/13/2013*	*Citric*	*2 months*	*4*[b]
AL 6063-T52	1/9/2014	Citric	OCP	3
AL 6063-T52	*3/10/2013*	*Sulfamic*	*2 months*	*4*[a]
AL 6063-T52	2/11/2014	Sulfamic	OCP	3
AL 6063-T52	12/14/2012	Baseline	N/A	

[a] First treatment performed immediately before exposure. Removed on 9/24/14.

[b] First treatment performed immediately before exposure. Removed on 11/4/14.

Table 4.3-2. Current acid treatment samples in WSW.

Sample	Exposure Date	Acid	Interval	# of Treaments
AL 6063-T52	*9/13/2013*	*Citric*	*2 months*	*6*[a]
AL 6063-T52	*9/13/2013*	*Sulfamic*	*2 months*	*6*[a]
AL 3003 HT	7/23/2013	Citric	2 months	6[b]
AL 3003 HT	7/23/2013	Sulfamic	2 months	6[b]
AL 6063T52	10/19/2012	Baseline	N/A	
AL 3003 HT	7/23/2013	Baseline	N/A	

[a] First treatment performed immediately before exposure. Removed on 7/25/2014.

[b] First treatment performed after 2 months of exposure.

Initial trials used 10% (v/v) sulfamic acid with a treatment interval of either every two months or every six months. In CSW, this concentration may have accelerated pitting, both samples were removed after 5 months of exposure. The sulfamic treatment concentration has now been adjusted to 5% (v/v), resulting in a solution with pH = 1.3. Test 46 is treated on a two-month interval while Test 45 is treated based on OCP.

In Test 46, the sample OCP rose to the steady state value of the baseline sample (~ -720 mV) within 45 days, almost three months sooner than the baseline sample. After the two-month treatment, OCP dropped to ~ -1000 mV but immediately began to increase. OCP reached and remained at -720 mV two weeks prior to the four-month treatment. The four-month treatment dropped OCP to ~ -1000 mV, but OCP returned to -720 mV within 30 days. Corrosion product was observed on the trailing edge of the sample after two months. The sample was removed on 9/24/14.

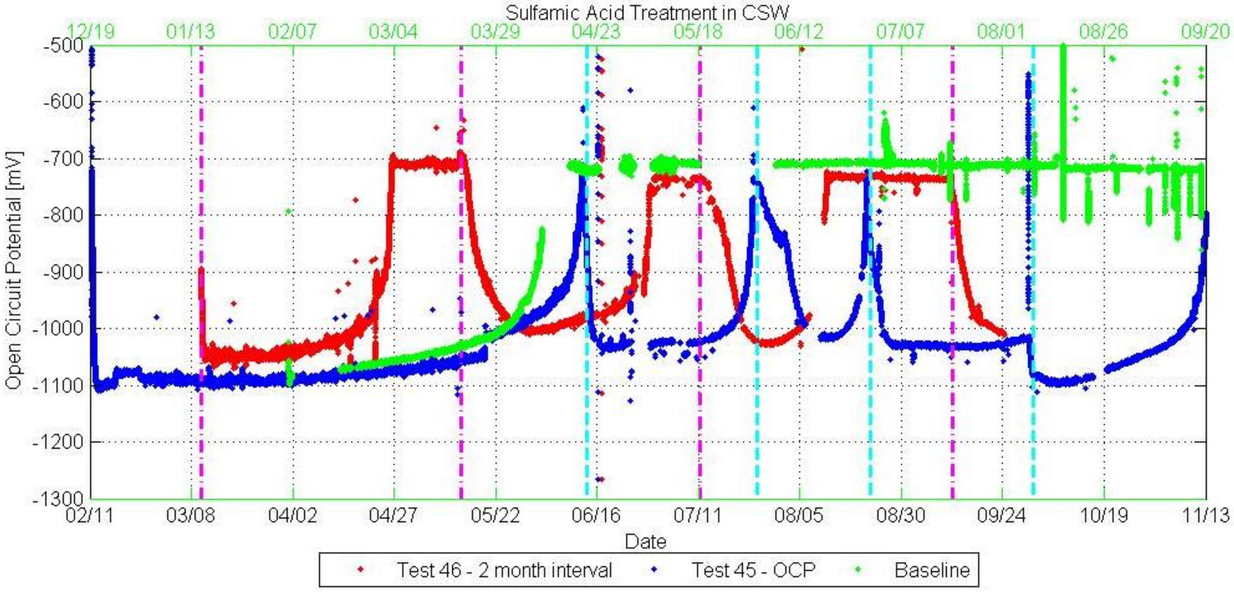

Figure 4-13. Sulfamic acid treatment in CSW. Test 46 2-month treatment dates are indicated by magenta lines and Test 45 OCP-based treatment dates are indicated by cyan lines. Only the first 275 days of exposure are shown for the baseline coupon (actual date is on upper x-axis in green). Treatments have been successful in lowering OCP to ~ -1000 mV. Test 45 was in stagnant fresh water for several hours due to a flow disruption on 10/1/14.

In Test 45, the OCP has followed the baseline sample, reaching -700 mV after 120 days, when it was given the first treatment. After the first treatment, OCP remained ~ -1020 mV for 30 days before beginning to increase rapidly. The second treatment was performed 40 days after the first treatment. After the second treatment, OCP was lowered to -1000 mV but began increasing immediately. The second treatment lasted for 7 minutes instead of the standard 2 minutes. The third treatment was performed 30 days after the second treatment. OCP after the third treatment is currently steady at ~ -1020 mV.

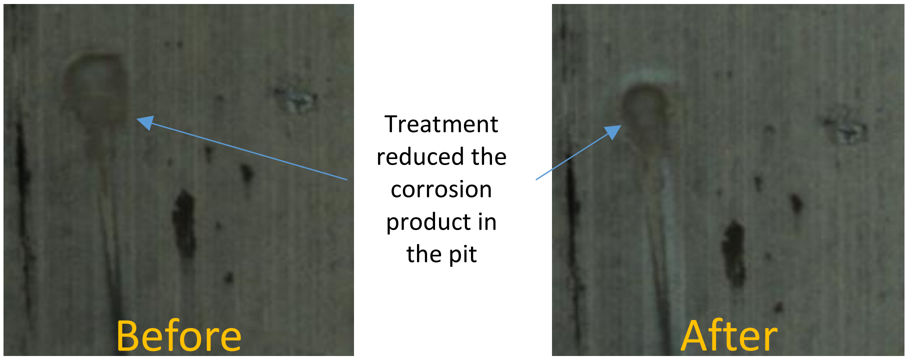

Figure 4-14. Before and after sulfamic treatment. Corrosion product buildup was lessened in this pit, but result was not observed for all pits.

Some reduction in corrosion product buildup was observed post-treatment for some pits (Figure 4-14) but not all pits. Removal of corrosion product is believed to prevent the development of localized environments which could further accelerate pitting.

Citric acid treatments also utilize a 5% (v/v) concentration, which results in a solution with pH = 2.8.

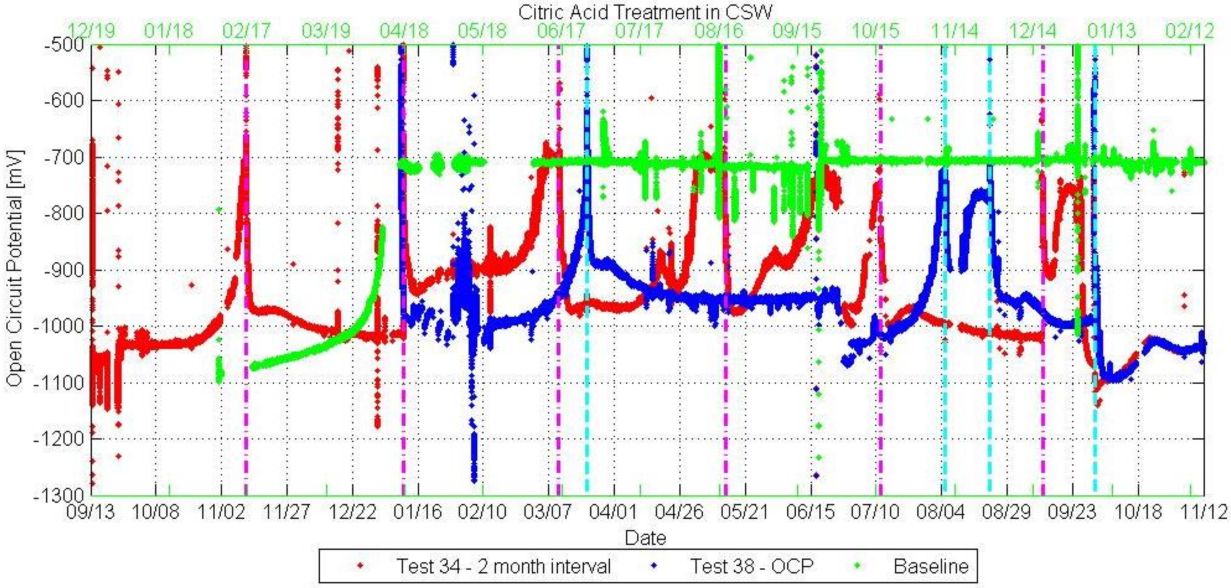

Figure 4-15. Citric acid treatments in CSW. Test 34 2-month treatment dates are indicated by magenta lines and Test 38 OCP-based treatment dates are indicated by cyan lines. Only the first 425 days of exposure are shown for the baseline coupon (actual date is on upper x-axis in green). Treatments have been successful in lowering OCP to between -900 mV and -1000 mV. Test 38 was in stagnant fresh water for several hours due to a flow disruption on 10/1/14.

For Test 34, the first treatment was given just prior to starting CSW flow. The two-month treatment coincides with OCP starting to rise towards pitting potential. Although this is ~60 days faster than the baseline sample, the treatment suppressed OCP to below the baseline sample. The four-month treatment resulted in an OCP above the pre-treatment value. OCP continued to rise until it reached OCP of the baseline sample, where it remained until the six-month treatment (~10 days). After the six-month treatment OCP dropped below the pre-treatment value and slowly began to increase after 40 days. Pits on the trailing edge of the sample and some corrosion product buildup were observed at eight months of exposure Figure 4-16). The eight-month treatment dropped OCP but it began to rise immediately. The ten-month treatment dropped OCP and OCP remained around -1000 mV until the twelve-month treatment. The sample was removed on 11/4/2014. The pits that were observed at eight months do not appear to have worsened.

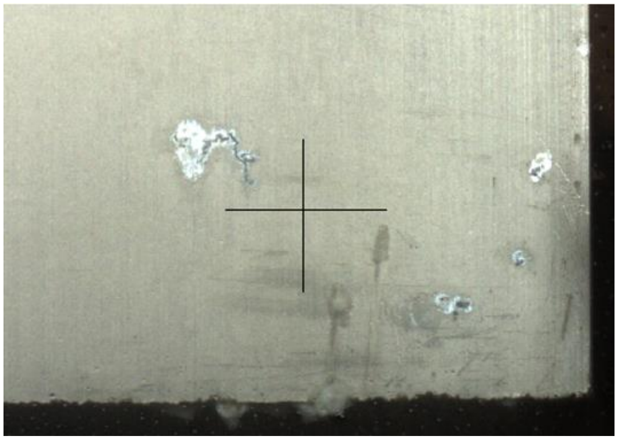

Figure 4-16. After eight months of exposure, pits and corrosion product buildup were observed on the trailing edge of the sample receiving citric acid treatment every two months.

For Test 38, OCP rose to the pitting region after 60 days, nearly two months faster than the baseline sample. The time between each treatments has been different; treatments have been separated by two months, four months, and two weeks.

In WSW, all samples, including the baseline sample, have OCP below -900 mV (Figure 4-17). Samples were removed on 7/25/14 due to space constraints. No significant observations on treatment effects could be made.

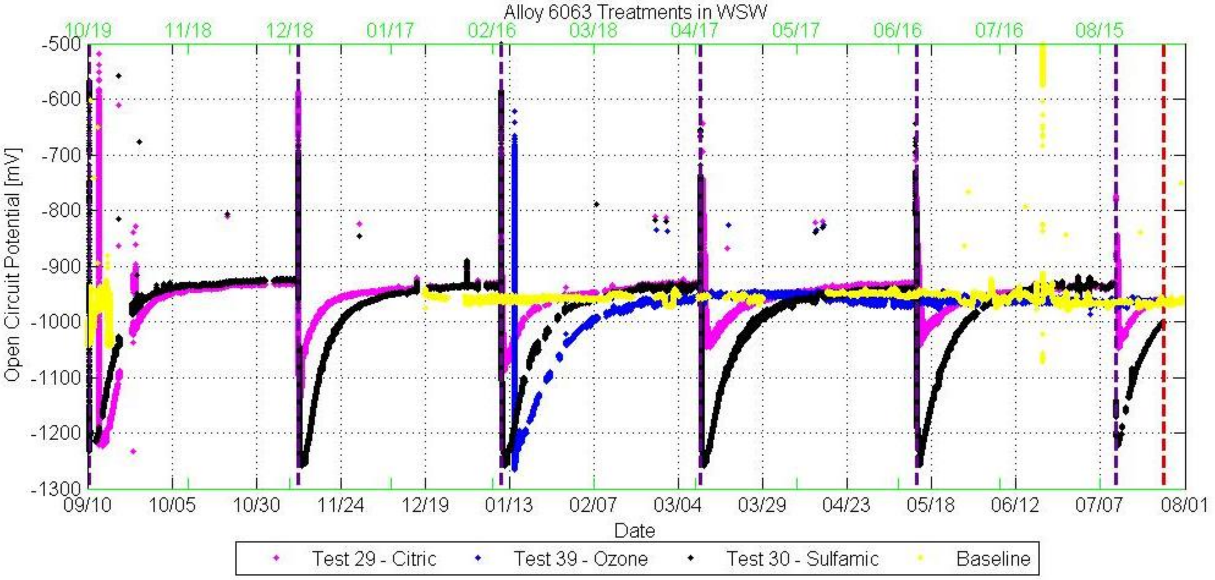

(a) Alloy 6063-T52 coupons in WSW. Treatment intervals are 2 months; dates are indicated by purple dashed lines. No ozone treatment was performed on 3/14/2014. Only first 325 days of exposure are shown for the baseline coupon (actual date is on upper x-axis in green). Treatment coupons were removed on 7/25/2014 (red line). Baseline coupon is still installed.

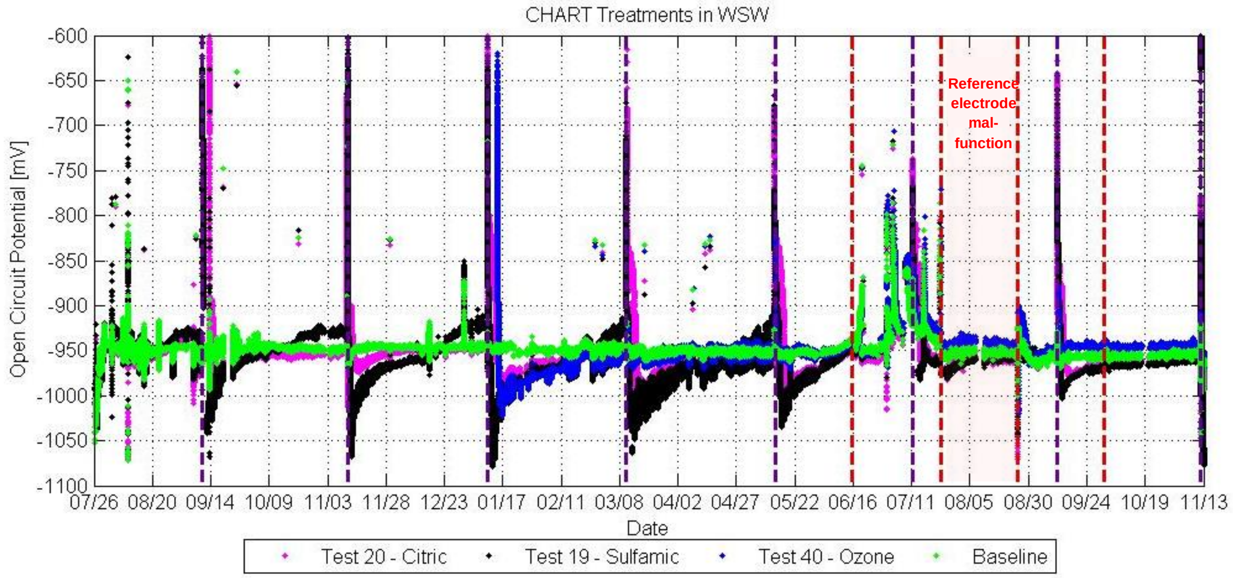

(b) CHART samples (heat treated Alloy 3003). Treatment intervals are 2 months; dates are indicated by purple dashed lines. No ozone treatment was provided on 3/14/14. OCP measurements between 6/15/14 – 7/23/14 (pink shaded box) should be ignored due to malfunctioning reference electrode. Flow disruption on 8/23/14 and 10/1/14 (third and fourth vertical red lines) resulted in samples being held in stagnant freshwater for several hours.

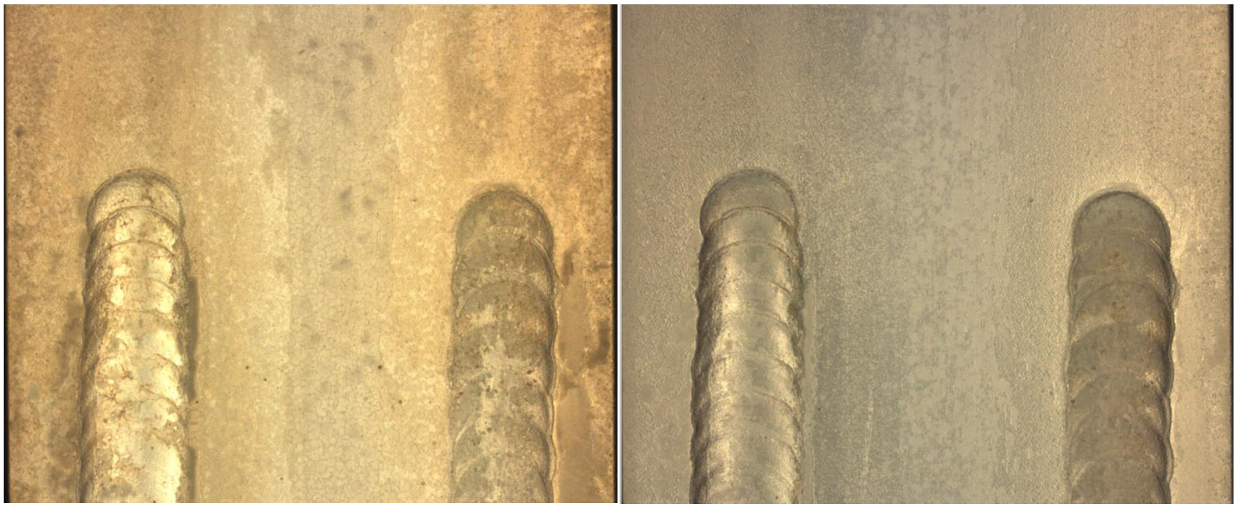

(c) During sulfamic acid treatment on 11/11/14, the bio-slime layer peeled off the surface of the CHART coupon, resulting in changes in color and a cleaner coupon surface.

Figure 4-17. Acid and ozone treatments in WSW.

One difference between treatments in WSW vs. CSW lies in the post-treatment OCP. In WSW, sulfamic acid treatments and ozone drive OCP to ~ -1200 mV. The first citric acid treatment drove OCP to -1200 mV but subsequent treatments resulted in less negative OCPs. After the fourth citric acid treatment, OCP only reached -1050 mV, 100 mV less than the steady state OCP. In CSW, the post-treatment OCP is approximately the same each time.

4.4. OZONE TREATMENT

Makai is comparing the performance of samples given no treatment, one initial treatment, and multiple treatments on scheduled intervals.

The ozone treatment system is a Water Zone 10 by Ozone Solutions Inc. This unit can produce 10 gram/hour with its built-in 12 SCFH oxygen concentrator and compressor. Ozone injection into seawater is accomplished with a 3/4 HP March magnetic drive water recirculation pump feeding an MK-784 venturi injector. An ambient ozone sensor will signal the controller to shut the unit down in case of ozone leaks. Currently ozone treatment is available for samples tested in the MCIR and biofouling rack.

Initial results from the ozone treatment indicate accelerated pitting in ozone treated samples. Prior studies indicate ozone treatment is beneficial in developing a thicker, denser, oxide layer, which should provide better corrosion resistance. The appropriate ozone concentration, treatment time, and treatment interval are under investigation. The current treatment protocol recirculates ozonated water (1 ppm concentration) for 15 minutes per sample.

In CSW, one sample is being treated every 2 months. Similar to the acid treated samples, OCP of ozone treated sample reached ~ -700 mV almost 90 days earlier than the baseline sample (Figure 4-18). Small pits were observed 45 days after exposure. The two-month treatment was mistakenly missed and the four-month treatment was intentionally skipped to observe pit development. The six-month treatment was provided on 7/11/2014. The sudden drop in OCP on 6/26/2014 coincides with the removal of a steel sample from the MCIR.

The sulfamic and ozone pre-treatment sample was removed on 8/20/2014. No treatments were performed after the initial treatment (sulfamic acid at 10% for 2 minutes, ozonated CSW at 1 ppm for 15 min). OCP reached ~ -700 mV 70 days earlier than the baseline sample. Pits were observed after four months of exposure and by removal, the surface was covered in pits.

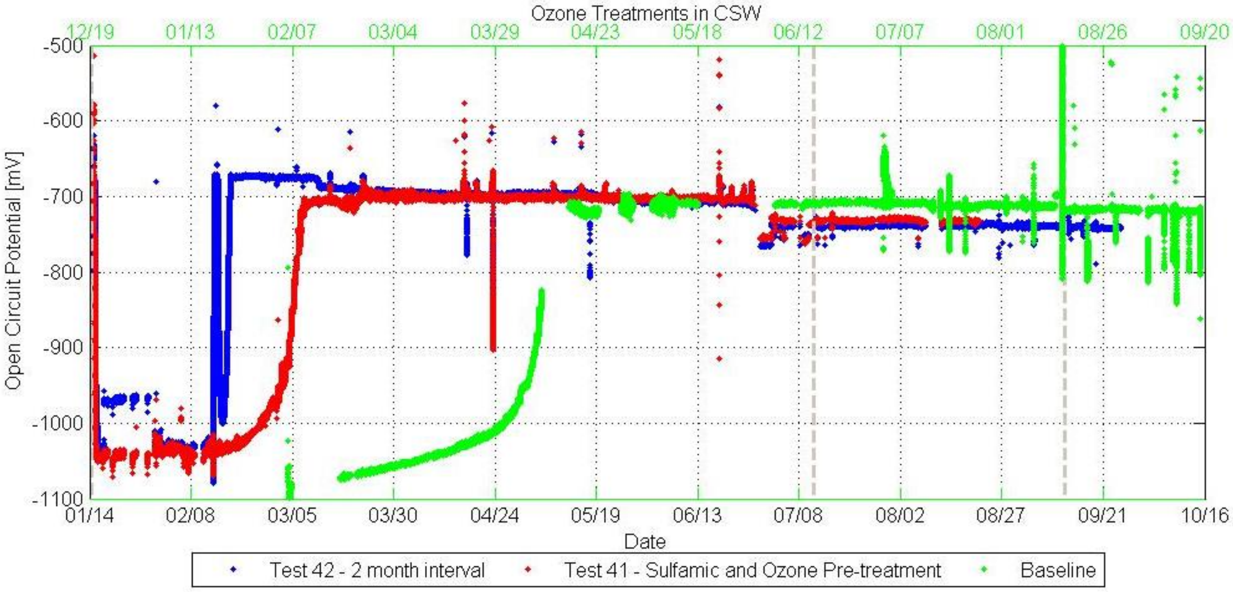

Figure 4-18. OCP of ozone treated samples reached steady-state 70 days (Test 41) and 90 days (Test 42) before the baseline sample. Ozone treatment dates for Test 42 are indicated by vertical gray lines. Treatments were planned but not performed on 3/10/2014 and 5/13/2014. Small pits were observed on 2/25/2014. Only first 275 days of exposure are shown for the baseline coupon (actual date is on upper x-axis in green). Test 41 was removed on 8/20/2014 and Test 42 was removed on 9/24/14.

In WSW, the samples treated with ozone appeared no different than the acid or baseline samples (Figure 4-17). Alloy 6063 samples were removed due to space constraints but CHART samples remain. No significant observations of ozone treatment effects can be made at this time.

Of the acid treatments tested, treatment intervals based on OCP have been more effective at preventing pitting compared to treatments based on set intervals for samples in CSW. Ozone treatments have not provided any pitting prevention or protection for the CSW samples.

4.5. CREVICE CORROSION/COATINGS

Previous testing on representative heat exchanger coupons demonstrated extensive crevice corrosion at the gasket interface. Since these connections are not critical heat transfer surfaces, suitable coatings could be applied to protect the interface without impacting heat exchanger performance. Alodine 1201, SiloXel, and 3M 5200 were investigated. Alodine 1201 is a chromic acid based chemical that produces a chrome conversion coating which becomes part of the aluminum surface. It has been used to improve corrosion resistance in marine applications, but contains hexavalent chromium which is environmentally hazardous and requires treatment prior to disposal. SiloXel is a quasi-ceramic conversion coating for aluminum developed at the University of Hawaii. 3M 5200 is a polyurethane marine adhesive/sealant that is marketed to resist weathering and salt water.

Samples of Alloy 3003 and Alloy 6061 were tested along with three coatings to test: Alodine, SiloXel, and 3M 5200. Two additional coating combinations, 3M 5200 applied to Alodine or SiloXel coated samples only at the gasket interface, were also tested. Including the untreated control sample, 6 configurations per alloy were tested.

In general, SiloXel coating integrity was unreliable. Several samples exhibited coating failures as shown in Figure 4-19.

Figure 4-19. Typical SiloXel coating defect on in-line plate. Samples were still tested.

4.5.1. In-Line Test

The in-line test replicates heat exchanger seawater-side connections. The flow of seawater is perpendicular to the metal-gasket interface. In-line test samples are tested as a unit and were exposed to WSW and CSW in February 2013. Performance assessment was limited to visual inspection of the outside surfaces while the unit was being tested. WSW and CSW units were opened for interior inspection after one year.

No corrosion was observed in WSW, which is consistent with results from representative heat exchanger testing. Little information pertaining to coating efficacy could be gathered without any corroding samples; the WSW test was decommissioned in February 2014.

The CSW unit was decommissioned in March 2014, after 13 months of exposure. Corrosion was present in all samples except for Alloy 3003 coated with SiloXel and sealed with polyurethane. Corrosion occurred in the flow channel, starting from the metal-gasket interface, or on the outside edge of the gasket (Figure 4-20). Coatings provided some degree of protection. For Alloy 6063, Alodine, Alodine with polyurethane, and SiloXel with polyurethane had at least one sample that was free of corrosion. For Alloy 3003, all the control and polyurethane coated samples had corrosion; all other coating combinations protected at least one sample from corrosion.

The variability in coating performance may impact the feasibility for use in OTEC heat exchangers. For example, the discrepancy between the performance of SiloXel with polyurethane applied to Alloy 3003 versus 6063 may be attributed to defects in the coating process rather than the performance of the coating itself.

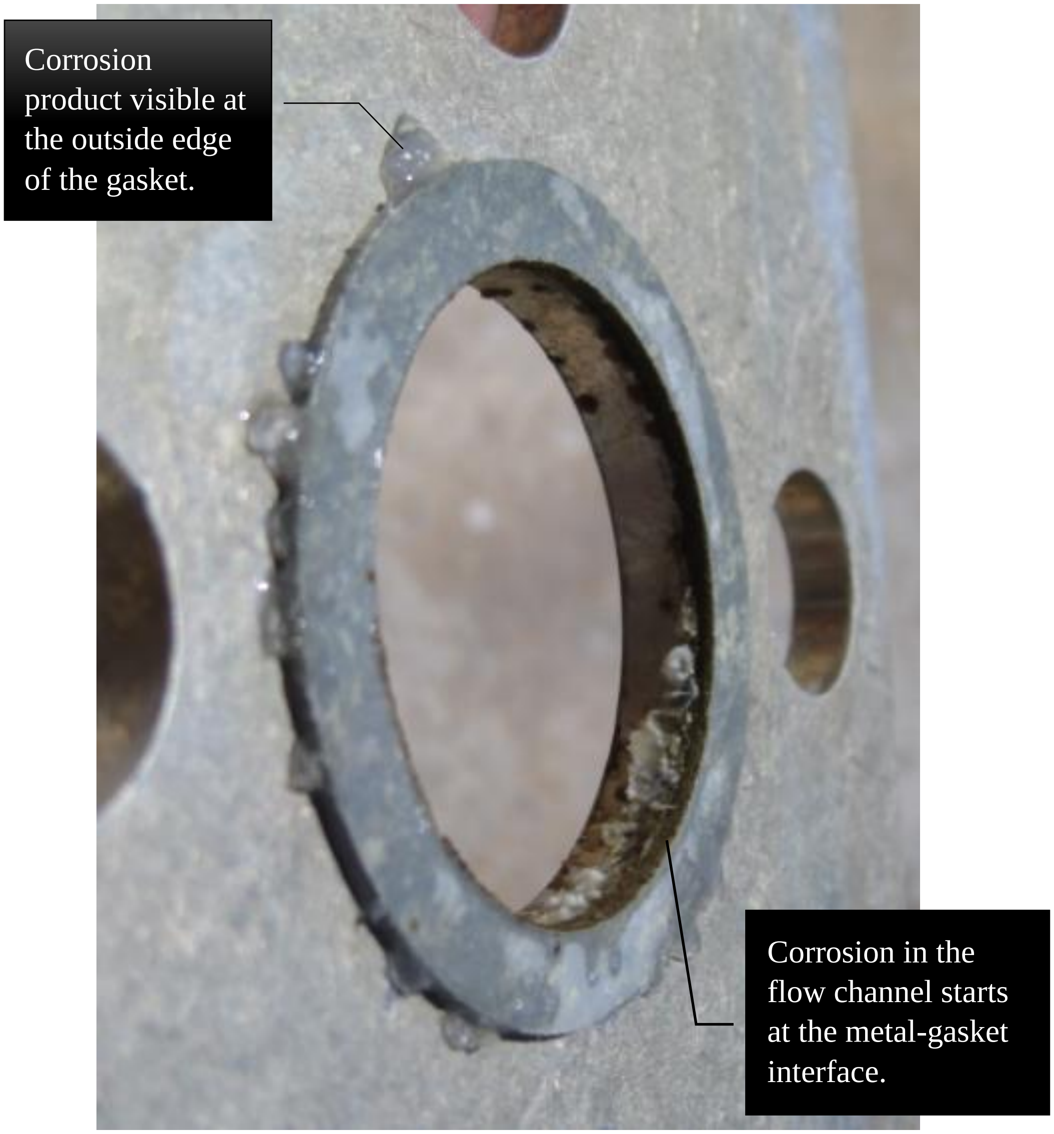

Figure 4-20. In-line sample showing corrosion in the flow channel starting at the metal-gasket interface and on the outside edge of the gasket.

4.5.2. Cross-Flow Test

The cross-flow test replicates conditions within a plate and frame heat exchanger. The flow of seawater is parallel to the metal-gasket interface. Cross-flow test samples were tested in the three-point racks and were exposed to WSW and CSW in January 2013. Photographs were used to assess sample performance.

No corrosion was observed in WSW, which is consistent with results from representative heat exchanger testing. Little information pertaining to coating efficacy could be gathered without any corroding samples; the WSW test was decommissioned in February 2014.

The CSW unit was decommissioned in March 2014, after 13 months of exposure. Results were similar to the in-line test samples. For Alloy 3003, only the control and polyurethane coated samples were corroded at the metal-gasket interface. The Alodine and Alodine with polyurethane samples were not corroded at the metal-gasket interface but showed some corrosion at the edge of the coupons. Only the SiloXel and SiloXel and polyurethane samples were free of corrosion across the entire sample. For Alloy 6063, the control and polyurethane coated samples were severely corroded at the metal-gasket interface and pits covered ~ 60% of the sample surface. Only the SiloXel with polyurethane coating prevented corrosion at the metal-gasket interface in all the samples. The remaining coating combinations had one or two samples that still had corrosion.

Similar to the in-line test, the variability in coating performance may impact the feasibility for use in OTEC heat exchangers.

4.6. BIOFOULING

Biofouling negatively impacts heat exchanger performance by reducing the heat transfer coefficient and, in severe cases, impeding flow channels. Biofilms can also create local environments that can accelerate corrosion. Makai has been using hypochlorination for one hour each day for biofoulant control. Since studies using ozone and iodine treatment have been promising, Makai decided both warranted further investigation.

The iodine treatment system and protocol was provided by I2 Air Fluid Innovation, Inc. The system uses an air compressor to force air through cartridges filled with iodine resin. Iodine vapor is entrained in the air and delivered into the water stream via air bubbles. Iodine treatment testing was performed on a custom rack.

Iodine infusion testing was inconclusive. Although the testing continued over several months, equipment malfunctions made it unlikely adequate iodine vapor was entering the system. The major issues were: 1) seawater backflow into the iodine resin cartridges and 2) light exposure. Moisture in the cartridges interferes with the entrainment of iodine vapor as air is forced through the cartridge. Although samples were drawn during infusion, they were sent out for analysis; the concentration was not determined in real-time and any issues with concentration were not identified until much later. The equipment complexities could be resolved, but algal fouling is likely at OTEC intake locations and may travel into the heat exchanger. Algae can grow even with low level light exposure. Iodine is an anti-bacterial; the biocidal action is not effective on algae. At this time we will focus on investigating biocides that eliminate algae as well as bacteria.

The ozone treatment system is the same as used in pitting mitigation studies. The original system has been modified to deliver ozonated seawater to the biofouling rack.

Hypochlorination is achieved by using a Chemtech metering pump to pump bleach into the WSW inlet header for one hour each day. Recent studies in health and water quality industries emphasize adjusting biocide treatments based on oxidation reduction potential (ORP) rather than concentration. An ORP around 600 mV provides disinfection whereas an ORP around 800 mV provides sterilization. A hypochlorite concentration of 550 ppb yields an ORP of 750 mV. The metering pump has been adjusted to deliver 550 ppb for one hour each day and ORP will be monitored periodically to determine if further adjustments are required (changes in water quality could require more or less bleach to achieve the same ORP).

Based on ATP and bacterial plate count results, the current hypochlorination treatment is effective in controlling biofouling. Although testing in the 1980's found a chlorine concentration of 70 ppb was sufficient to control biofouling, our testing found a 250 ppb hypochlorite concentration did not increase ORP above 400 mV, well below the 600 mV required for disinfection and the 800 mV required for sterilization. Hypochlorination level is now adjusted to reach a desired 750 mV in ORP. ORP changes natural fluctuations in water chemistry, but, in general, a concentration of ~ 550 ppb is required to establish 750 mV.

Ozone treatment may also provide effective biofoulant control, but treatment should be more frequent than once a month. ATP test results from the biofouling test indicate ozone provides immediate sterilization (low RLU in the ozone treated samples when swabbed within an hour of treatment) but fouling begins after the treatment is over (high RLU in ozone treated samples when swabbed 24 hours after treatment). Furthermore, once a biofilm is established, it is difficult for any type of treatment to be 100% effective. Bacteria and microbes can use the film as a protective barrier. One caution to the use of ozone is that in preliminary tests of ozone treatments in CSW (1 ppm for 5 min, every two months), samples have shown accelerated localized corrosion. Test duration and sample sizes have been small so it is difficult to draw conclusions about the effect of ozone on pitting but corrosion must be taken into account when selecting biofoulant controls.

ATP, bacterial plate count, and photographs of the interior surfaces of the samples in the biofouling rack confirm the efficacy of hypochlorite treatment at concentrations that raise ORP to ~ 750 mV for one hour daily.

5. CONCLUSION AND OUTLOOK

This period's accomplishments included testing two evaporators and a condenser. Titanium plate-frame type heat exchangers were tested. The APV condenser had high U values but also high seawater pressure drop. The APV evaporator had mid-range U values and very low seawater pressure drop. U-value was limited by ammonia-side convection, which changed very little with increasing duty. To date, based on corrosion and performance testing results, the optimum OTEC condenser still remains elusive. Makai is testing prototype versions of a new heat exchanger design and upcoming efforts will focus on working with manufacturing techniques to support full-scale, economical production of Makai's heat exchangers.

Corrosion testing is on-going. The five-year box coupon samples were removed in November 2014 and will be analyzed shortly. Steel testing has concluded and Makai is no longer pursuing steel as a potential heat exchanger material. Coating testing has also concluded. Additional work in coatings has not been planned for heat exchange surfaces but coatings have potential to protect non-heat transfer surfaces such as tubesheets and manifolds. Acid and ozone treatment testing will continue. The biofouling study concluded bleach was the most effective treatment but some accumulation of slime still coats sample surfaces. Modifications to the bleach system are planned to incorporate monitoring during bleach delivery, finer control of bleach concentration, and flexibility to treat CSW in addition to WSW. Corrosion efforts will continue to target pitting and biofouling prevention/mitigation treatments. Makai plans on using advancements made this year in Makai's ultra-sonic monitoring capability to provide better assessment of treatment performance.

A major portion of Makai's efforts will be focused on turbine operations and understanding the power generation intricacies of an OTEC system. Turbine installation is underway and turbine testing is slated for early 2015. The next step would be developing controls so OTEC-generated electricity could be provided to the grid.

Finally, since Makai's vision for OTEC's future is in off-shore facilities, Makai also has development work planned for cost effective cold water pipe construction and installation solutions.